

QC944

~~75~~  
~~TSL~~

1074-15

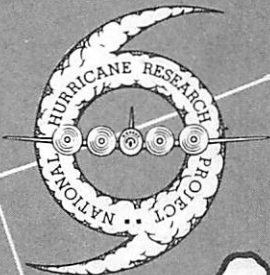
N39  
no. 15  
ATSL

# NATIONAL HURRICANE RESEARCH PROJECT

REPORT NO. 15

## The Three-Dimensional Wind Structure Around a Tropical Cyclone

ATMOSPHERIC SCIENCE  
LABORATORY COLLECTION





U. S. DEPARTMENT OF COMMERCE  
Sinclair Weeks, Secretary  
WEATHER BUREAU  
F. W. Reichelderfer, Chief

NATIONAL HURRICANE RESEARCH PROJECT

REPORT NO. 15

# The Three-Dimensional Wind Structure Around a Tropical Cyclone

by

Banner I. Miller

Weather Bureau Office, Miami, Fla.



Washington, D. C.  
January 1958



U18401 0606248

## NATIONAL HURRICANE RESEARCH PROJECT REPORTS

Reports by Weather Bureau units, contractors, and cooperators working on the hurricane problem are pre-printed in this series to facilitate immediate distribution of the information among the workers and other interested units. As this limited reproduction and distribution in this form do not constitute formal scientific publication, reference to a paper in the series should identify it as a pre-printed report.

- No. 1. Objectives and basic design of the National Hurricane Research Project. March 1956.
- No. 2. Numerical weather prediction of hurricane motion. July 1956.  
Supplement: Error analysis of prognostic 500-mb. maps made for numerical weather prediction of hurricane motion. March 1957.
- No. 3. Rainfall associated with hurricanes. July 1956.
- No. 4. Some problems involved in the study of storm surges. December 1956.
- No. 5. Survey of meteorological factors pertinent to reduction of loss of life and property in hurricane situations. March 1957.
- No. 6. A mean atmosphere for the West Indies area. May 1957.
- No. 7. An index of tide gages and tide gage records for the Atlantic and Gulf coasts of the United States. May 1957.
- No. 8. Part I. Hurricanes and the sea surface temperature field. Part II. The exchange of energy between the sea and the atmosphere in relation to hurricane behavior. June 1957.
- No. 9. Seasonal variations in the frequency of North Atlantic tropical cyclones related to the general circulation. July 1957.
- No. 10. Estimating central pressure of tropical cyclones from aircraft data. August 1957.
- No. 11. Instrumentation of National Hurricane Research Project aircraft. August 1957.
- No. 12. Studies of hurricane spiral bands as observed on radar. September 1957.
- No. 13. Mean soundings for the hurricane eye. September 1957.
- No. 14. On the maximum intensity of hurricanes. December 1957.
- No. 15. The three-dimensional wind structure around a tropical cyclone. January 1958.

QC944  
.N39  
NO. 15  
ATSL

THE THREE-DIMENSIONAL WIND STRUCTURE AROUND A TROPICAL CYCLONE

Banner I. Miller  
WBO Miami, Fla.

[Manuscript received August 7, 1957; revised December 7, 1957]

ABSTRACT

Wind data from a number of hurricanes are combined to obtain a composite picture of the hurricane circulation. Several layers from the surface to 16 km. are investigated. Divergence, vertical motion, and vorticity are computed from the mean data for the various layers. The results are discussed in relation to current models of the hurricane circulation.

1. INTRODUCTION

In 1952 E. Jordan [2] and Hughes [1], constructed composite pictures of the wind circulation for selected levels around a tropical cyclone. Since that time the number of wind observations made in the vicinity of tropical cyclones, particularly in the Atlantic area, has been greatly increased. The use of a larger number of wind observations might reveal some additional features of the hurricane circulation. The present investigation was designed (1) to extend the works of E. Jordan and Hughes by making use of the later accumulation of data; (2) to investigate the mean circulation by deep layers instead of at selected levels. The layers selected for study were the 0-1, 1-3, 3-6, 6-10, 10-12.5, and 12.5-16-km. layers.

2. SELECTION AND AMOUNT OF DATA

All data used were from Atlantic storms. The requirements for inclusion in the data tabulations were: (1) The central pressure of the storm was 985 mb. or lower; (2) the center of the storm at the time the wind observation was made was south of 35°N. Latitude; (3) the rawin balloon reached an elevation of at least 6 km.

All reports that met the above requirements and fell within a grid covering 12° of latitude ahead of and behind the center of the storm and 8° to the right and left of the direction of motion were tabulated. The grid is shown in figure 1. The hurricane is at the center of the grid, which moves with the storm. The size of the grid was deliberately chosen to exceed that of the average hurricane in order that the mean flow just outside the vortex circulation might be investigated in relation to the storm's motion. The results of the latter will be made the subject of a later report.

Most of the observations were made in conjunction with hurricanes Hazel

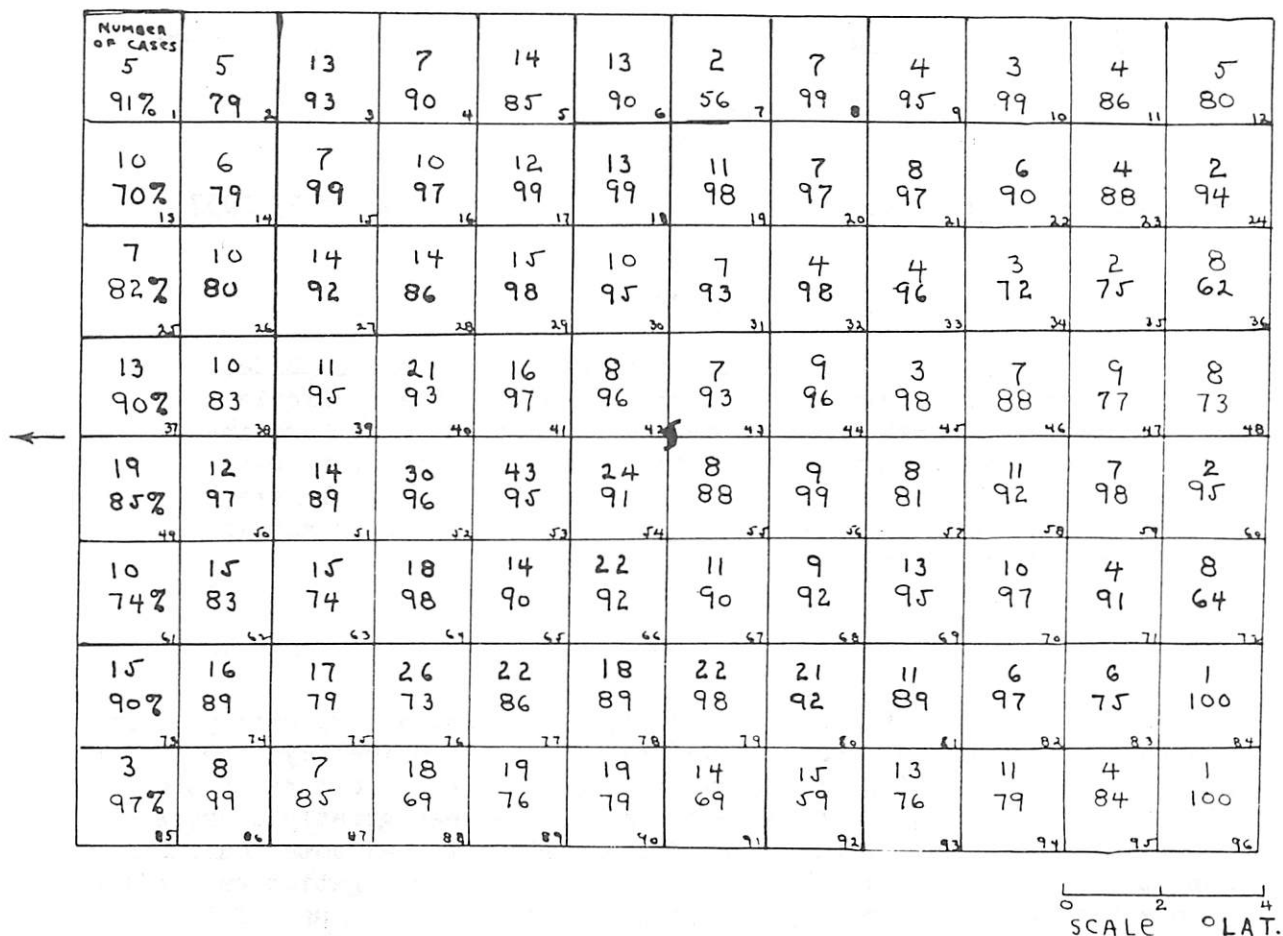


Figure 1. - Grid used in data tabulation. Number of observations at 6 km is shown in center of each square, with persistence percentage below it. Key number of square is in lower right corner. Arrow at left in this and subsequent illustrations shows direction of motion of storm.

1954; Connie, Diane, Ione, Janet 1955; and Betsy 1956. After these data were tabulated, some areas of the grid were left with few observations. Therefore, it became necessary to supplement the data by reports from other storms dating back to 1946. These were selected primarily with the view in mind of filling in the blank areas; the three basic requirements listed in the first paragraph of this section were, however, observed. The number of observations, tabulated by 2° squares, is shown in figure 1. The total at 6 km. was 1047. This decreased to 659 at 16 km. E. Jordan [2] used about 130 wind reports in the lower layers and 88 at 45,000 feet; Hughes [1] processed about 500 individual wind observations. The grid used in the present study, however, is somewhat larger than that used by either Jordan or Hughes.

Geographically, the observations were made at stations along the Atlantic and Gulf coasts of the United States, through the islands in the Caribbean, Bermuda, the Bahamas, and Central America. Most of the observing stations were south of 35°N., the exceptions being Washington, D. C., Norfolk, Va., and Hatteras and Greensboro, N. C. Most of the data were obtained while

the center of the hurricane was still at sea, although the fact that the center was going inland did not automatically eliminate the inclusion of the observation as long as the other requirements were met. August, September, and October storms were used primarily, although a few observations from June hurricanes were tabulated. All data were plotted by  $2^\circ$  squares relative to the center of the storm. The arrow at the left of figure 1 (and subsequent illustrations) indicates the direction of motion of the storm.

### 3. DETERMINING THE MEAN WIND FOR A LAYER

In working up a winds aloft observation, the usual procedure is to average the balloon travel over a 2-minute interval for the lower levels and a 2- to 4- minute interval for the higher levels. For example, the direction of the balloon from the observer at the end of 2 minutes determines the wind direction for the first minute. The speed for the first minute is the horizontal distance of the balloon from the station divided by the time; i.e., two minutes.

Since it was the intent of this study to investigate the mean circulation by deep layers instead of by selected levels, a procedure similar to that used for evaluating the wind at the end of the first minute was applied to layers ranging from 1 km. to 10 km. in thickness. The original winds aloft records were obtained. The direction and horizontal distance of the balloon from the observer at 1, 3, 6, and 10 km., and the time of ascent were recorded. The mean wind direction for the 0-1, 0-3, 0-6, and 0-10-km. layers was assumed to be the direction of the balloon from the observer at the time it reached the top of the layer. The mean wind speed for the layer was the horizontal distance of the balloon from the observation point divided by the time of ascent.

This procedure is permissible because the balloon is a natural integrator [5] and

$$R = \int_{t_s}^{t_h} V dt \quad (1)$$

where  $R$  is the horizontal component of the vector connecting the observation point and the balloon at level,  $h$ , where the balloon is released at time  $t_s$ , and reaches the level,  $h$ , at time  $t_h$ .  $V$  is the horizontal wind velocity.

The individual wind observations were combined by procedures to be described in the next section and the averages for the various layers beginning at the surface and extending up to 10 km. were calculated. The average speeds were converted into distances by multiplying by the average time of ascent. The 0-1, 0-3, 0-6, and 0-10-km. layer averages were determined in this manner. To obtain the averages for the 1-3, 3-6, and 6-10-km. layers, the distances for each of the three lower layers were subtracted vectorially from those of the next higher layer. For example, the 0-1-km. distances were subtracted from the 0-3-km. distances, which gives the data needed to calculate the 1-3-km. mean layer winds.

This method of determining the averages for the intermediate layers was

adopted because the work involved in differentiating (by finite differences) the individual observational curves would have been prohibitive. However, it is probably permissible to work with averages since the data are completely homogeneous up to 6 km. and relatively so up to 10 km. The loss in total number of observations in going from 6 km. to 10 km. was less than 10 percent. Above 10 km. the number of observations dropped off rapidly. Therefore, prior to determining the mean areal winds for the two top layers (10-12.5 and 12.5-16 km.), individual winds were computed for these two layers by subtracting the individual 10-km. distances from the 12.5-km. distances, the 12.5-km. distances from the 16-km. balloon travel, etc.

#### 4. METHOD OF DETERMINING THE AREAL MEANS

Two methods of combining the data were used, one for the four inner squares (Nos. 42, 43, 54, and 55 in fig. 1), and another for the remainder of the grid. The latter method will be discussed first.

After the data tabulations were completed, the individual wind observations were added with the aid of the plotting board, and the mean was determined for each square. This mean was plotted at the center of the square.

The individual storm motions were averaged over a 12-hour period, 6 hours before and 6 hours after the time the wind observation was made. The composite mean motion for the entire grid was determined by weighting the individual storm velocities according to the number of wind observations taken at the time around which the individual storm motions were determined. For this group of data, the composite motion of the storms as determined above was 5.6 m.p.s, or about 11 kt. The average storm velocity, determined without weighting according to the number of observations, was almost identical, or 11.1 kt. The range of individual storm speeds was from 5 to 25 kt. Data for more rapidly moving storms, such as Hazel after it moved inland along the Carolina coast, were not used because of the large effect on the mean motion.

The mean storm motion for the entire grid (storm velocities for each square were not determined) was subtracted from the vector mean for each square. The radial and tangential speeds were computed graphically assuming as previously indicated that the mean properly belonged in the center of the square. The data for both components were smoothed by plotting the average for four adjacent squares at the intersections of those squares. Below 10 km. very little smoothing was required and this procedure served principally as an aid in drawing the isotachs (by increasing the number of points). Above 10 km. more smoothing was necessary. The motion of the storm was subtracted from the wind vectors before the components were computed in order to facilitate the smoothing of the data and the fitting of curves to the tangential speeds, both of which it was anticipated would have to be done. After the smoothing process was completed, the radial and tangential components were recombined with the motion of the storm to obtain the total wind field for each layer.

For the four inner squares (i.e., within a radius of about 2° of the center) it was necessary to combine the data in a somewhat different fashion for three reasons. First, the data were obviously biased in favor of weaker storms. Second, there was a greater concentration of observations in the outer portions of each square than there was near the center. Third, the direction of the

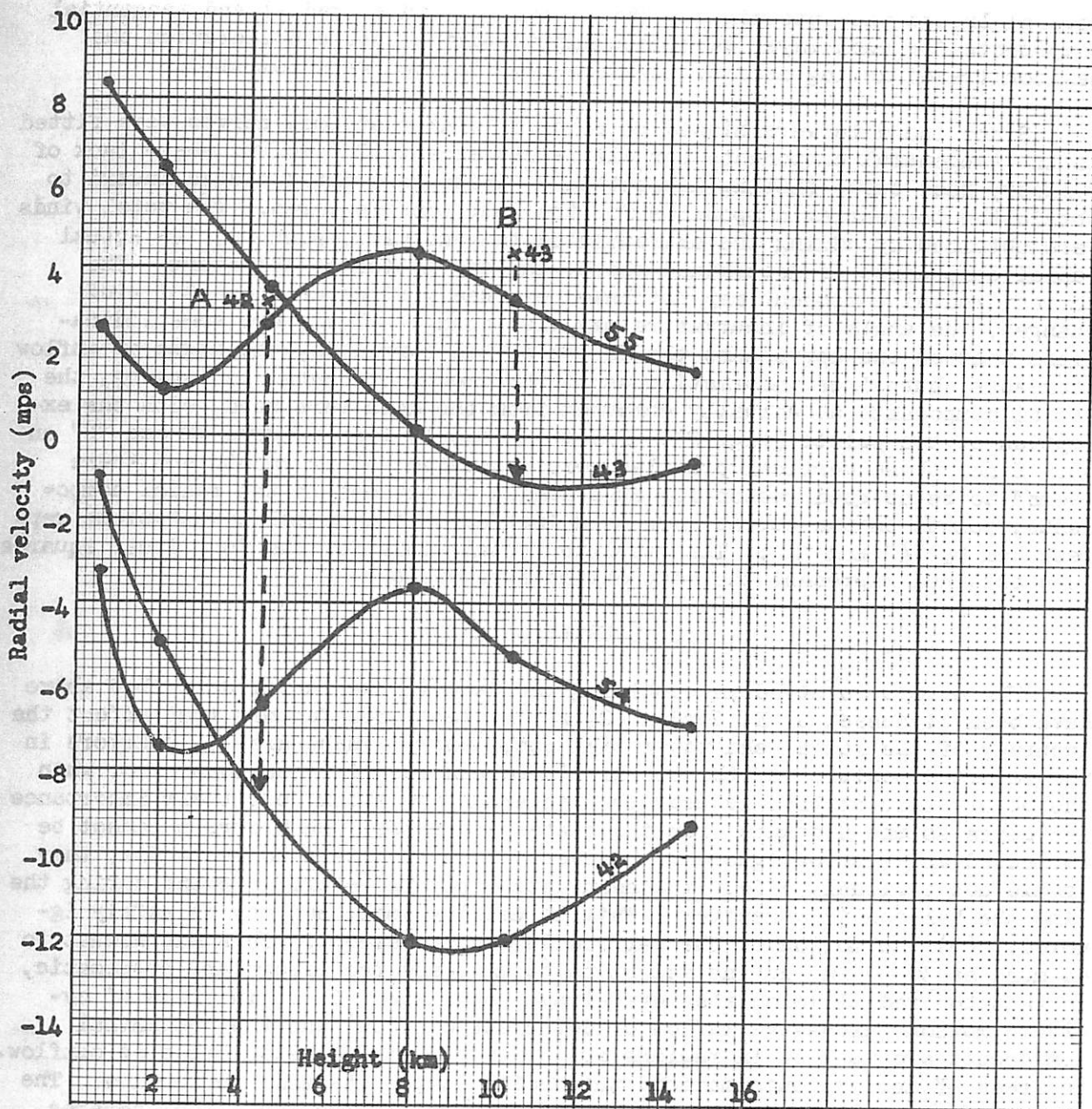


Figure 2. - Vertical profile of radial component for the four inner squares. (See fig. 1 for location of squares.)

tangential component varies  $90^\circ$  from one side of the square to the other. Consequently the data could not properly be placed at the center of the square.

Therefore, each individual observation was treated separately. First, the location of the observation station was plotted as a polar coordinate with the center of the storm at the origin. Second, in order to correct for the balloon travel during ascent, the location of the balloon in relation to the observation station was plotted at 1, 3...16 km., and the actual wind for the

several layers was determined. Third, the individual radial and tangential components for each layer were calculated, taking into consideration the balloon travel during ascent. Averages for the two were computed.

Since the data were biased in favor of weaker storms, curves were fitted to the tangential components for all layers except 12.5-16 km. where lack of symmetry made curve fitting impractical. These were extrapolated inward to obtain the tangential components for the four inner squares. The total winds were obtained by adding the extrapolated tangential components, the actual radial components as determined above, and the motion of the storm. The correct radial component may not have been used, since as the total wind changes, the angle of incurvature may also change. There are some indications that as one approaches the center of the hurricane, the angle of inflow decreases, but since information as to the amount of change is lacking, the radial components as actually computed from the data were used, with the exception of two points (fig. 2). Point "A" should lie on curve 42 and "B" on 43. Since these vertical profiles were otherwise rather smooth and there seemed to be no good reason for such sudden variations in the radial components, points on the curves were used instead of the actual computations represented by "A" and "B". The resulting total winds for the four inner squares thus obtained represent the best estimate possible.

#### 5. SOURCES OF ERROR

The errors involved in combining the data in the manner described above have been discussed by E. Jordan [2] who listed three factors that affect the accuracy of the radial and tangential components. These are: (1) Errors in the reported position of the storm. These can result in serious error when the observation station is near the center of the storm, but their importance decreases as the distance from the center increases. Such errors cannot be corrected and must be ignored. However, since they tend to be random, they should not seriously affect the mean data. (2) The storm movement during the time the balloon is ascending. This is usually small and may be safely ignored. (3) The motion of the balloon during its ascent. This may amount to as much as 30-50 km. during ascent to 16 km., and the errors are systematic, in that the radial velocities are always too large, (i.e., in areas of cyclonic motion, excessive inflow or deficient outflow) and the tangential components are too low in regions of inflow and too large in areas of outflow. In areas of anticyclonic motion, the radial components will be too low. The motion of the balloon has been corrected for within the four inner squares, but has been ignored elsewhere. First, the number of observations used made the work of replotting the individual observations for each layer prohibitive. Second, the size of the scale over which the data were averaged made such refinements appear unnecessary.

There are other possible sources of error in the present investigation. (1) The assumption that the data should be plotted at the center of the square. This would be true for a large sample and a random distribution of the observations within each square. The errors involved in working with a limited amount of data, however, should be random and may be largely eliminated by the smoothing process used. (2) The combination of data from storms of different size and intensity. Initially it was planned to use only data from storms

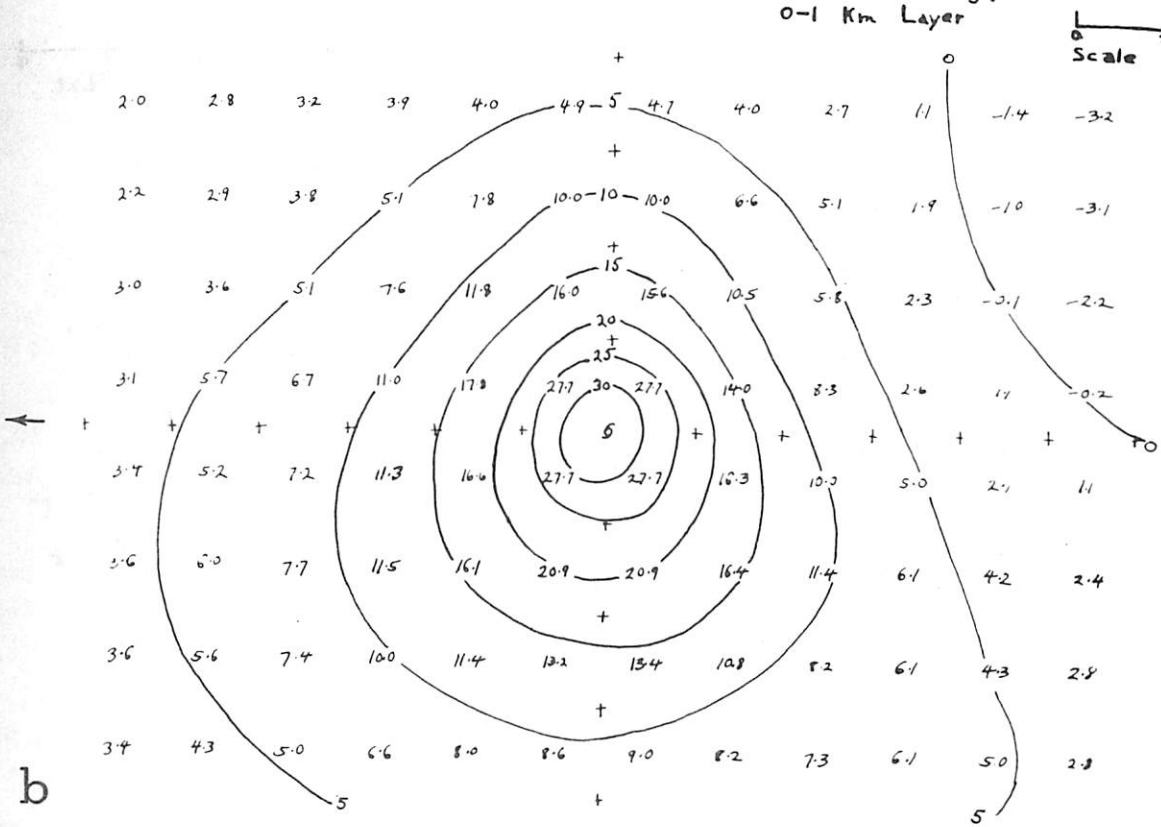
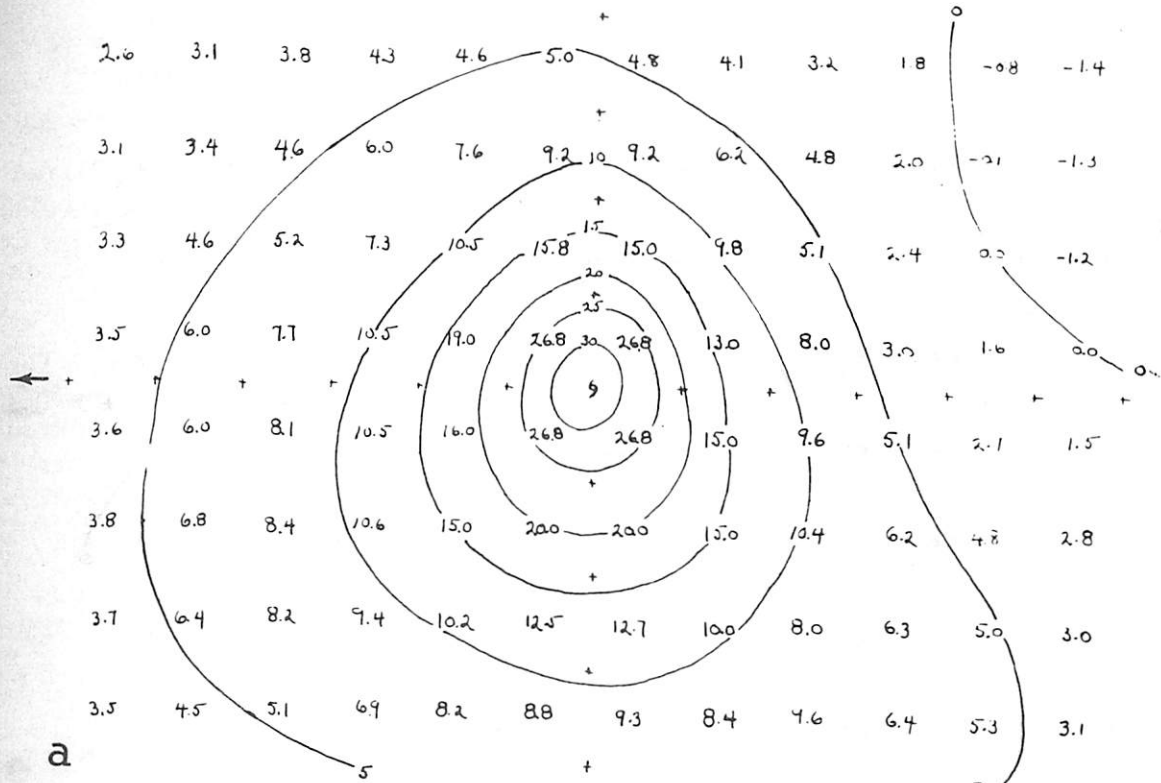


Figure 3. - Tangential speed (m.p.s.). Negative values indicate anticyclonic motion. Motion of storm has been removed.

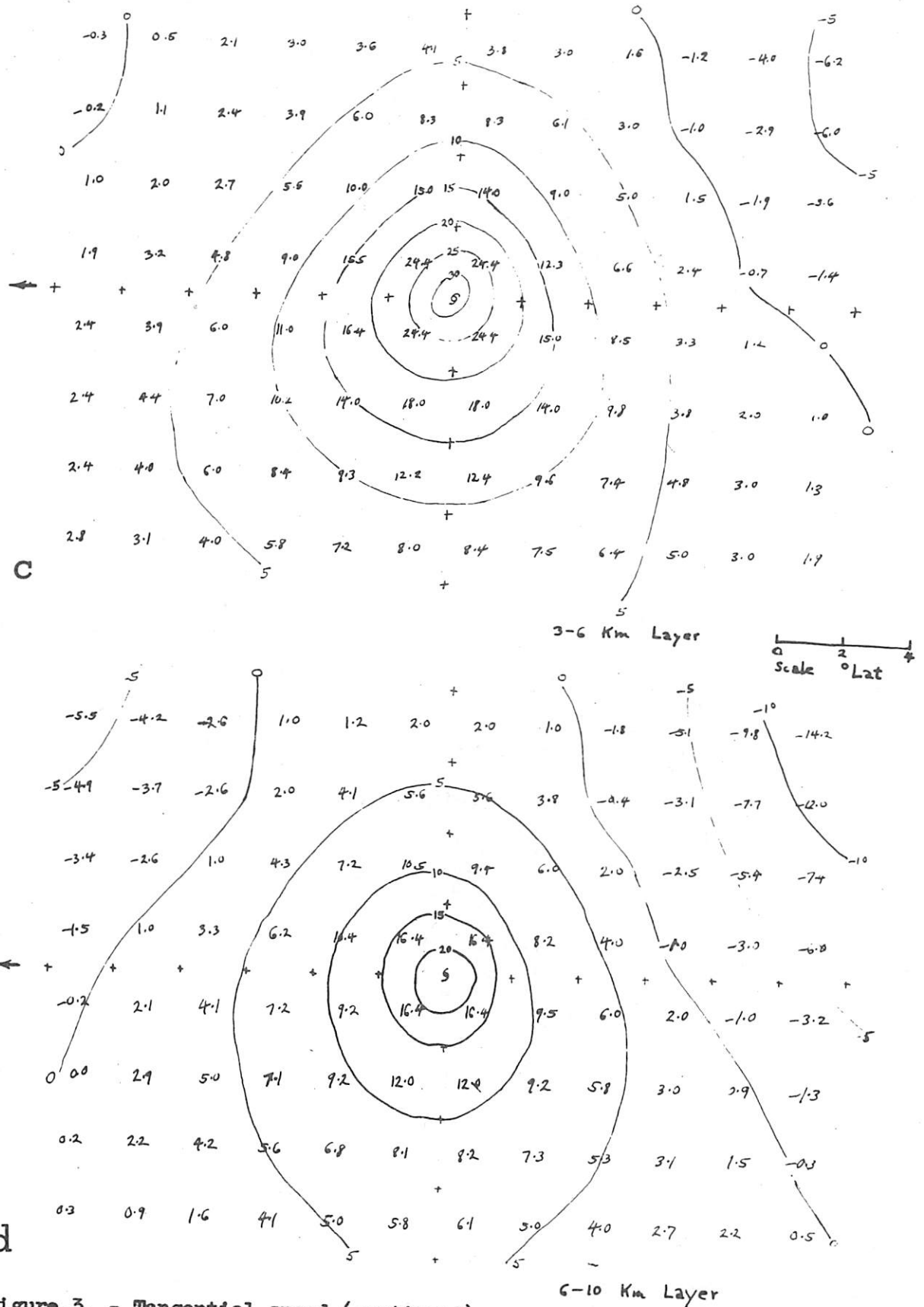


Figure 3. - Tangential speed (continued)

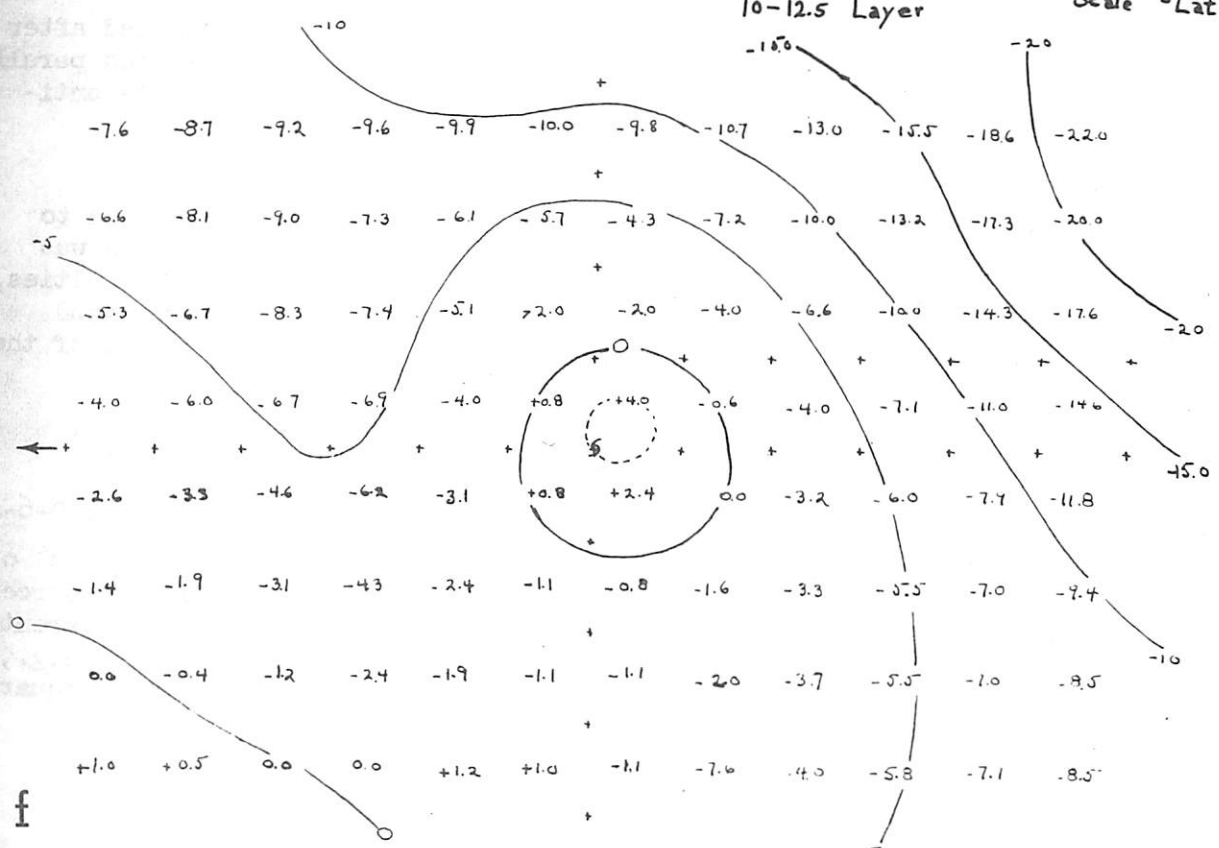
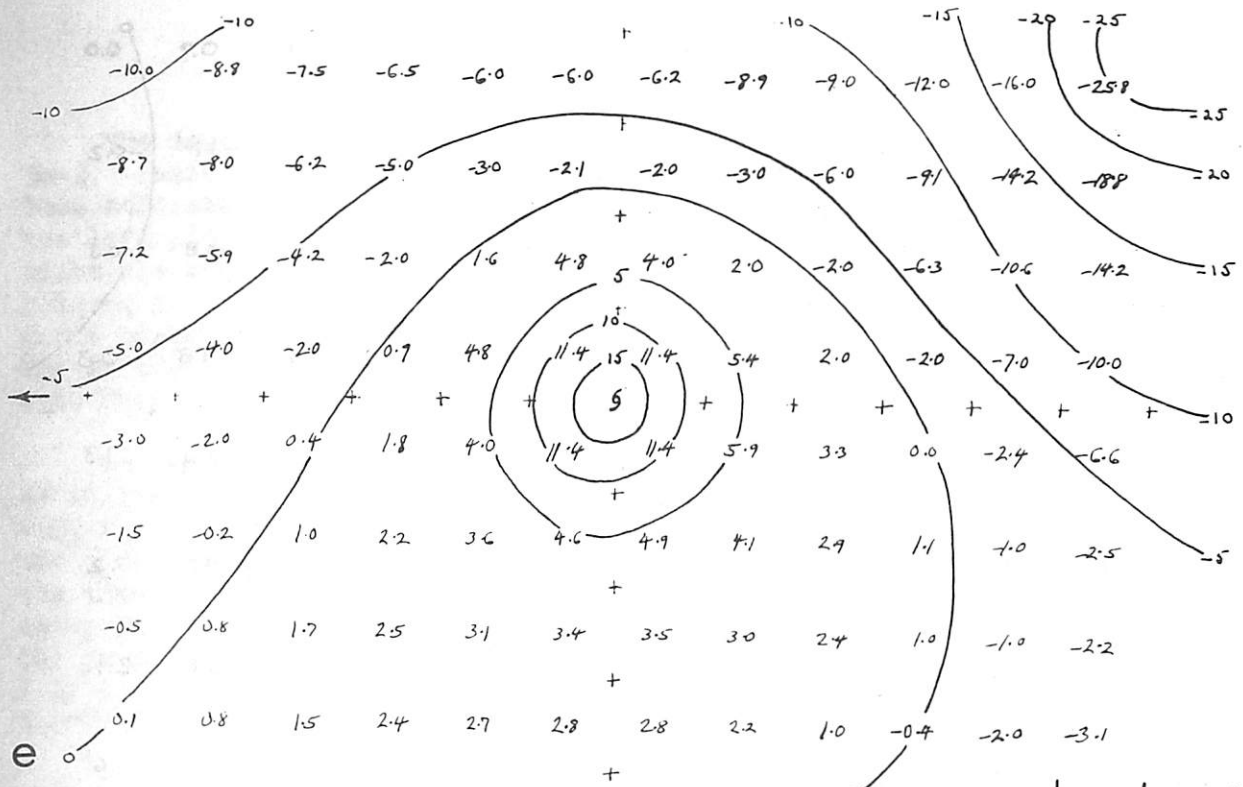


Figure 3. - Tangential speed (continued)

12.5-16 Km. Layer

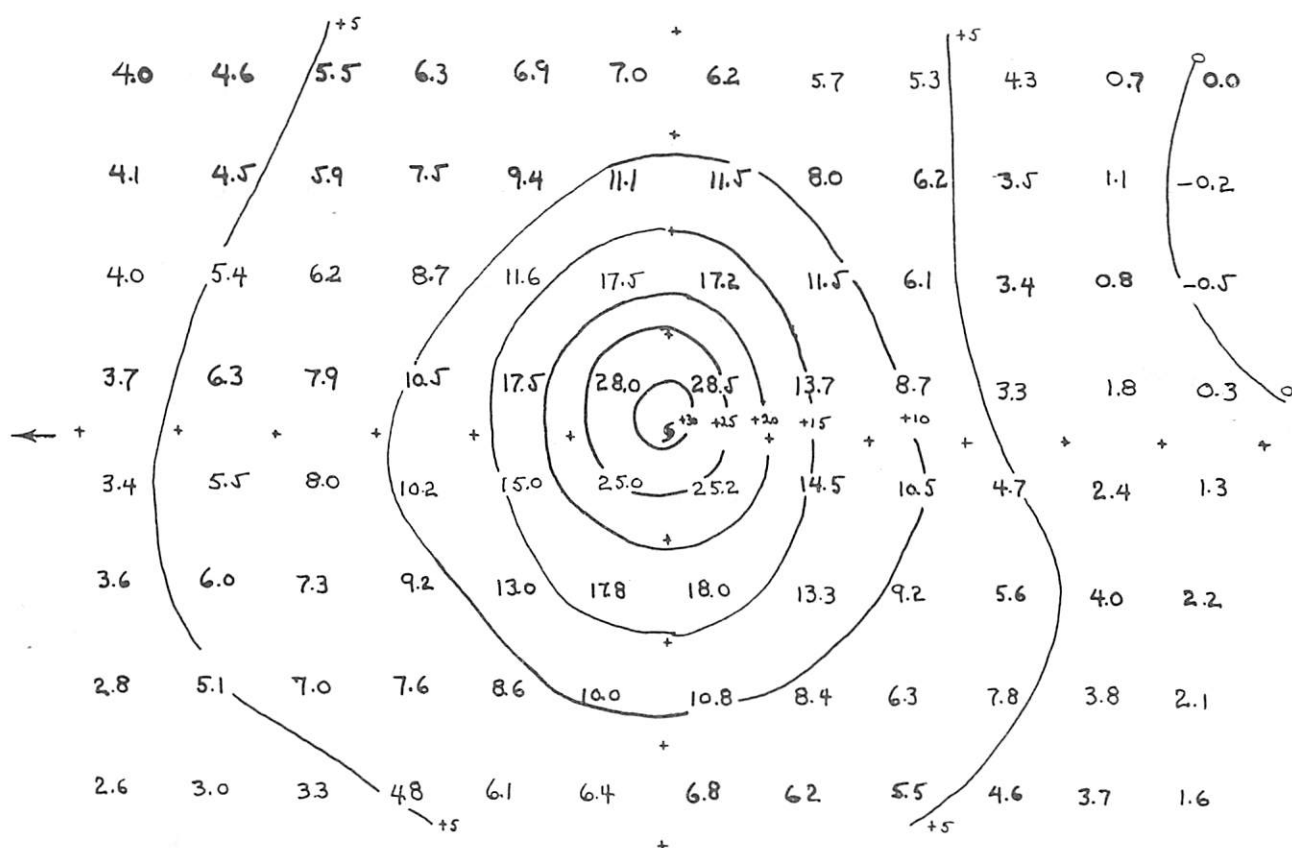


Figure 4. - Tangential speeds (m.p.s.) for the 0-1-km. layer obtained after subtracting from the mean wind the average component of the wind parallel to the direction of the storm motion. Negative values indicate anti-cyclonic motion.

with a central pressure of  $975 \pm 10$  mb. but there were not enough data to work with, and eventually data from all storms whose central pressure was 985 mb. or lower (ranging down to 914 mb.) were included. The difficulties, however, were not as great as had been anticipated. The mean layer wind directions were remarkably constant within a given square, regardless of the intensity of the storm. A persistence factor,  $\underline{P}$ , is defined as

$$P = \left( \frac{M_V}{M_S} \right) \times 100 \quad (2)$$

where  $\underline{M}_V$  and  $\underline{M}_S$  are the vector and scalar means respectively. For the 0-6-km. layer the persistence factors are shown in figure 1. Within about  $6^\circ$  of the center, most of these factors are sufficiently high (generally 90 percent or higher) to lend some support to the use of data from storms of different intensities. Some of these values are so high that they are suspect; e.g., 98 percent with 15 cases in square 29 and 98 percent with 18 cases in square 64; but they have been carefully checked and no errors can be detected.

## 6. THE TANGENTIAL COMPONENTS

The tangential components for the various layers are shown in figures 3a-f. These represent tangential speeds after the motion of the storm has been subtracted from the total wind field. The maximum values are found on the left side of the storm. This probably indicates that the data on the right are biased in favor of weaker storms, since it is easier to release a balloon in the left sector of the storm. That bias exists is, however, by no means certain. Another reason for the greater tangential speeds on the left may be that subtracting the full forward motion of the storm from the total wind over-corrects for the wind asymmetry due to the motion of the storm.

To test this possibility, the component of the 0-1-km. layer wind parallel to the motion of the storm was averaged over that part of the grid lying within  $6^\circ$  of the center. This was 3.2 m.p.s., compared to a mean motion of the composite storm of 5.6 m.p.s. This value (3.2 m.p.s.) was subtracted from the total wind field and the tangential wind speeds recomputed; these are shown in figure 4. The distribution of speeds is much more symmetrical about the center. This strongly suggests that much of the asymmetry of figures 3a-f is due to over-correction from subtracting the full forward speed of the storms from the total wind field.

Data for the lowest layer (0-1 km) reveals that anticyclonic motion exists within the right rear quadrant at a distance of about  $10^\circ$  from the center. This is outside the hurricane circulation. Most of the storms used in compiling the data were moving westward or northwestward. The anticyclonic portion of figure 3a, therefore, extends into the subtropical ridge.

The velocity profile for the lowest layer follows an exponential curve,

$$V_t = 37.6 e^{-.251r} \quad (3)$$

where  $V_t$  is the tangential speed in m.p.s.,  $r$  is the radial distance in degrees latitude, and  $e$  is the natural logarithmic base;  $r$  must be equal to or greater than the radius of maximum winds. This form of the profile has the disadvantage of not permitting any negative (anticyclonic) values.

The symmetry of the four tangential speeds about the center should not be taken literally. All these values, except the 12.5-16-km. layer, were obtained by extrapolating curves fitted to the data lying outside a radius of  $2^\circ$ . Figure 3f (12.5-16 km.) shows less symmetry as a whole than the lower layers do, and no attempt was made to fit a curve to these data. The tangential speeds around the center at this level represent the actual averages obtained from the data.

Inside a radius of about  $6^\circ$ , the tangential speeds are slightly higher through the 1-3-km. layer than they are for the 0-1-km. layer. Since all the data were collected from land stations, this may reflect the influence of friction through the first kilometer. Similar data over the open oceans might be different, but some retardation due to friction can be expected.

Above the 1-3-km. layer the tangential components decrease. The size of the cyclonic circulation (the area enclosed by the zero isotach) also shrinks. The magnitude of the anticyclonic motion in the right rear quadrant increases through the 10-12.5 km. layer and thereafter it drops off. There is some anticyclonic motion through the 3-6-km. layer along the extreme right front quadrant; this also increases through the 10-12.5-km. layer and then decreases.

Through the 10-12.5-km. layer there is still an appreciable area of cyclonic motion, although it is greatly displaced toward the left side of the storm. This is perhaps further evidence that the data are biased toward weaker storms on the right, or that subtraction of the full forward speed of the storm from the total wind over-corrects for the asymmetry due to the motion.

Through the 12.5-16-km. layer, the circulation is predominantly anticyclonic, although there is a small cyclonic center present on figure 3f. However, on the total wind field (fig. 11f) a closed circulation can no longer be detected.

The tangential velocity profiles for selected layers are shown in figure 5. These were obtained by averaging the values from figures 3a-f at 1° radial intervals 22.5° apart. The curves display a remarkable similarity in slope and general shape for all layers. The curve for the 12.5-16-km. layer shows that in the mean the motion is anticyclonic (negative values) outside a radius of about 2°.

## 7. THE RADIAL MOTION

Both total and relative radial components were computed. Total radial motion (figs. 6a-f) will be discussed first. Throughout the 0-1-km. layer the maximum inflow occurs in the right rear quadrant where it reaches a magnitude of about 9 m.p.s. Inflow is present throughout the entire rear portion of the storm. A small outflow is evident directly ahead of the storm. This pattern suggests that air is flowing through the storm. The next several layers (1-3 through 10-12.5 km.) are quite similar, although the inflow to the rear decreases and the outflow ahead of the storm increases in both area and magnitude. It may be of some significance that the area of maximum inflow shifts to the left rear at 10-12.5 km. and the maximum outflow to the right front. This also suggests that air is flowing through the storm, but that it is at different rates and from different directions at various levels. At the top of the storm (12.5-16 km.) almost the entire grid reveals outflow.

The vertical profiles of the radial components for the four inner squares are shown in figure 2. No reason is given for the hump on the two curves 54 and 55, both of which are to the left side of the storm. Since it occurs on each curve and at the same level, however, it is considered real. Whether or not it is of any significance is not entirely clear at this time.

The radial motion relative to the center of the storm is shown in figures 7a-f. In the lowest layer air is approaching the center from all quadrants except the left rear, where radial outflow is present. This outflow is also observed in the higher layers and appears to be real. The number of observations upon which the computations are based, figure 1, is large enough to

Tangential speed (mpe)

s  
p  
r  
s  
  
a  
6  
r  
t  
b  
r  
  
3  
i  
s

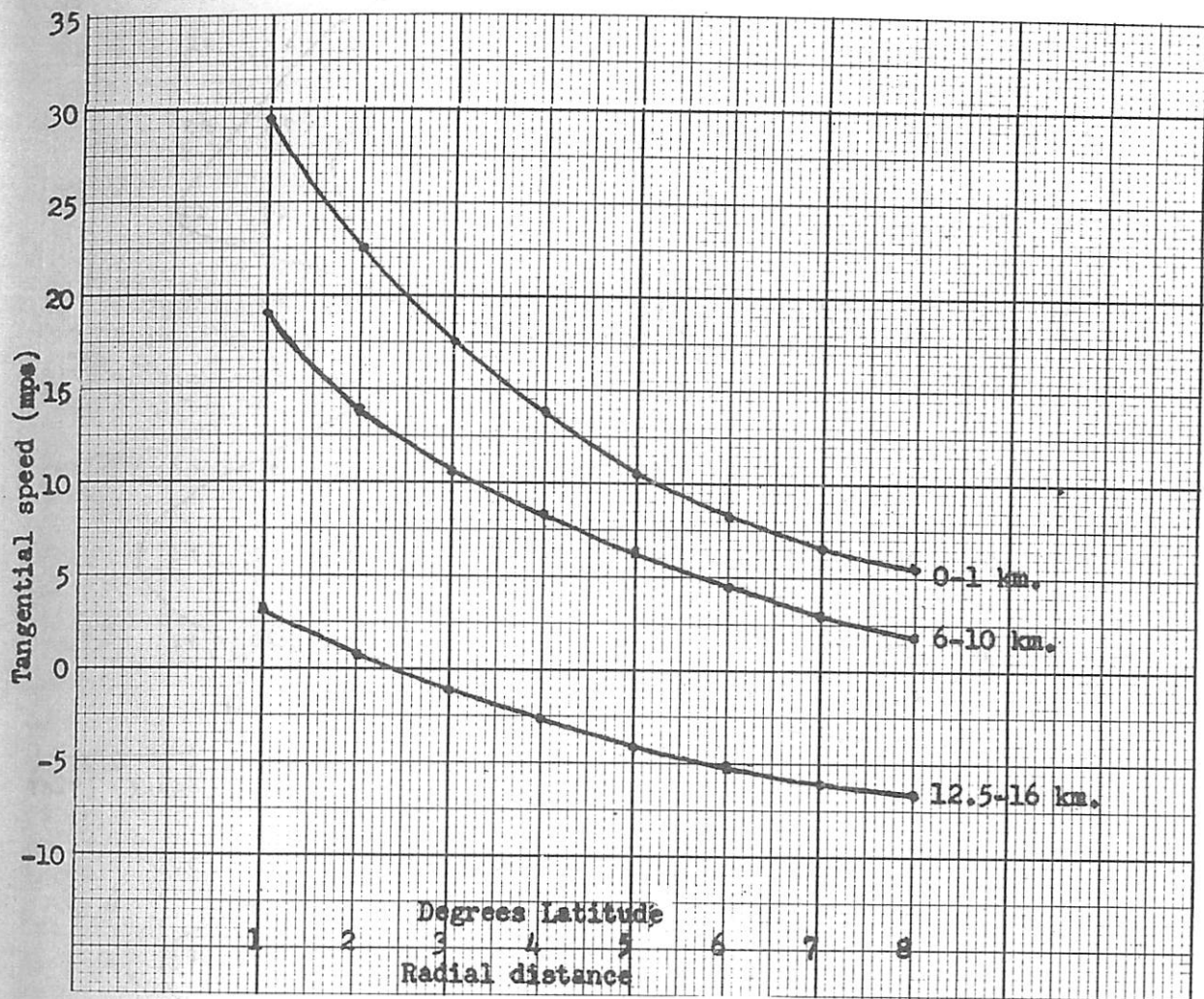


Figure 5. - Tangential wind profile for various layers

suggest that this outflow is typical. It does not appear possible that the process of combining the data could produce a fictitious picture of the radial motion within this one quadrant. This radial motion pattern also suggests that air is flowing through the storm.

The mean radial velocities for the two lowest and the two highest layers are shown in figure 8. These are based on the total radial motion (figs. 6a-f), but the results are the same as would have been obtained by use of the relative motion charts, since the subtraction of a constant (the motion of the storm) from the total wind field affects the distribution of the inflow but not the net radial component. The averages were computed from the values read at  $1^\circ$  intervals  $22.5^\circ$  apart.

The maximum inflow through the two lower layers occurs at a radius of  $3^\circ$ . Inside and outside that point there is a decrease in the inflow. This is at variance with the work of Hughes [1] whose radial velocity profile showed increasing inflow up to a radius of  $0.5^\circ$ .

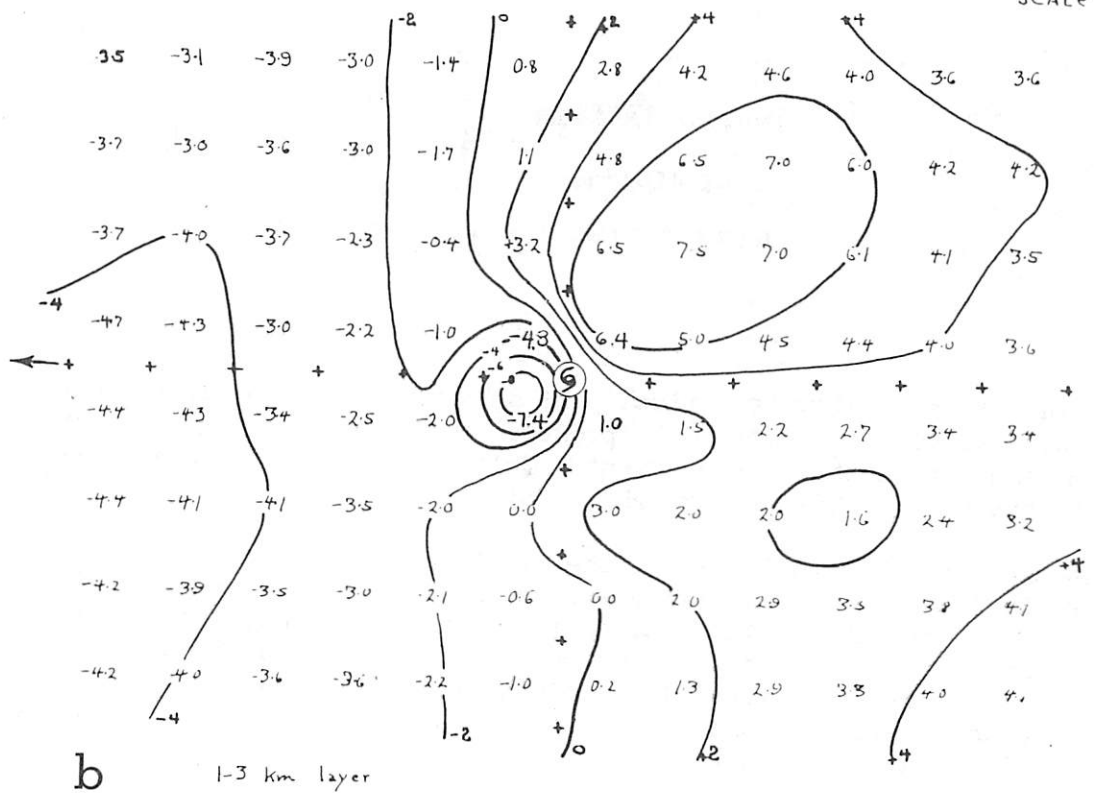
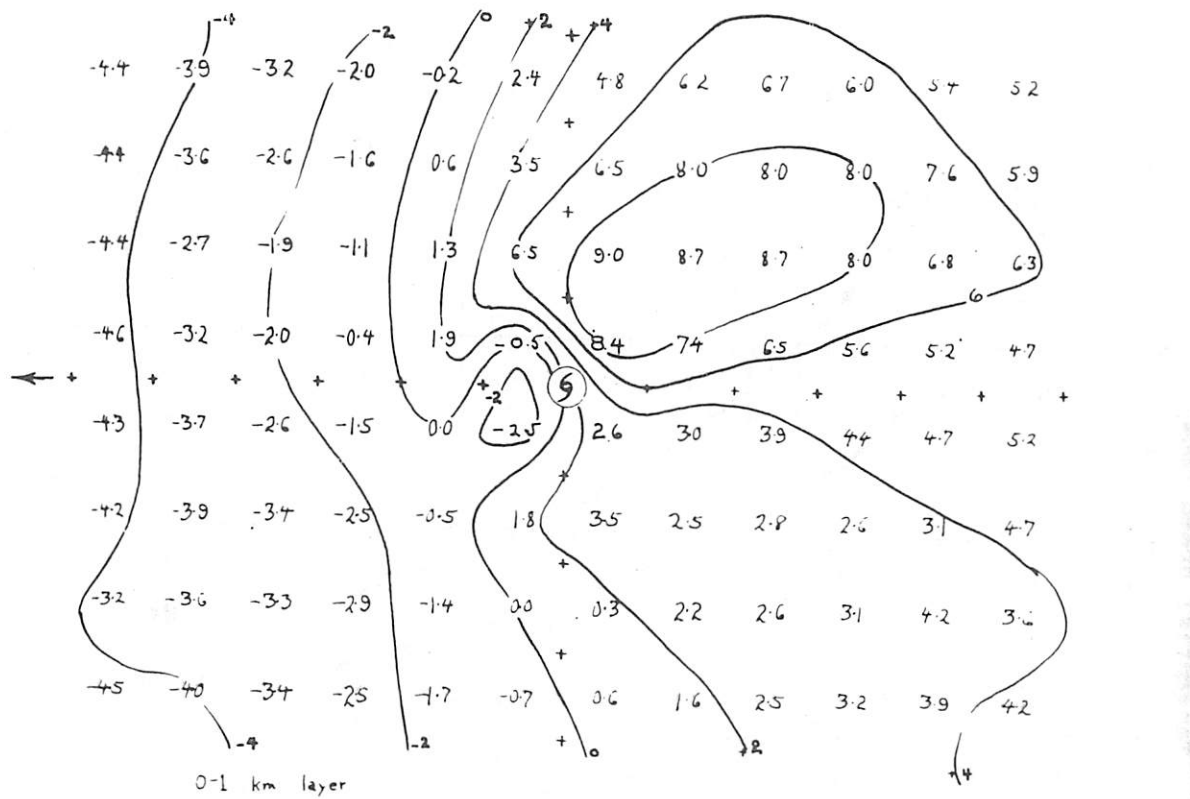
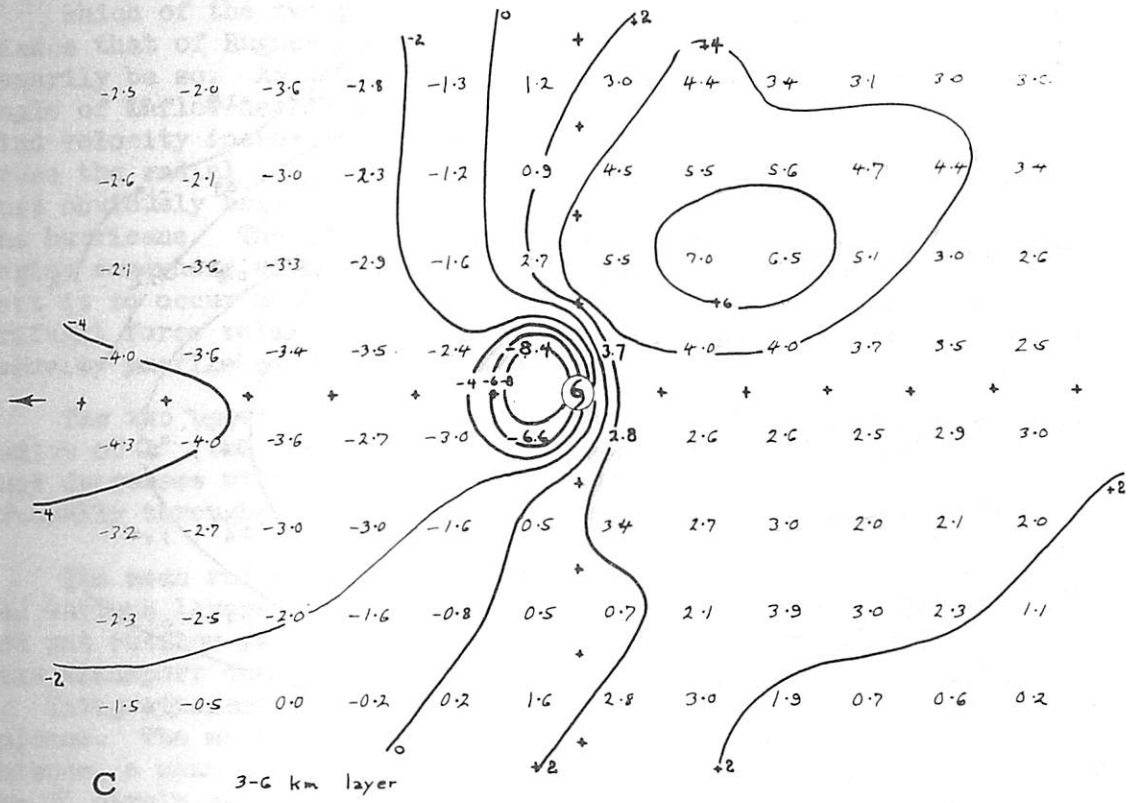
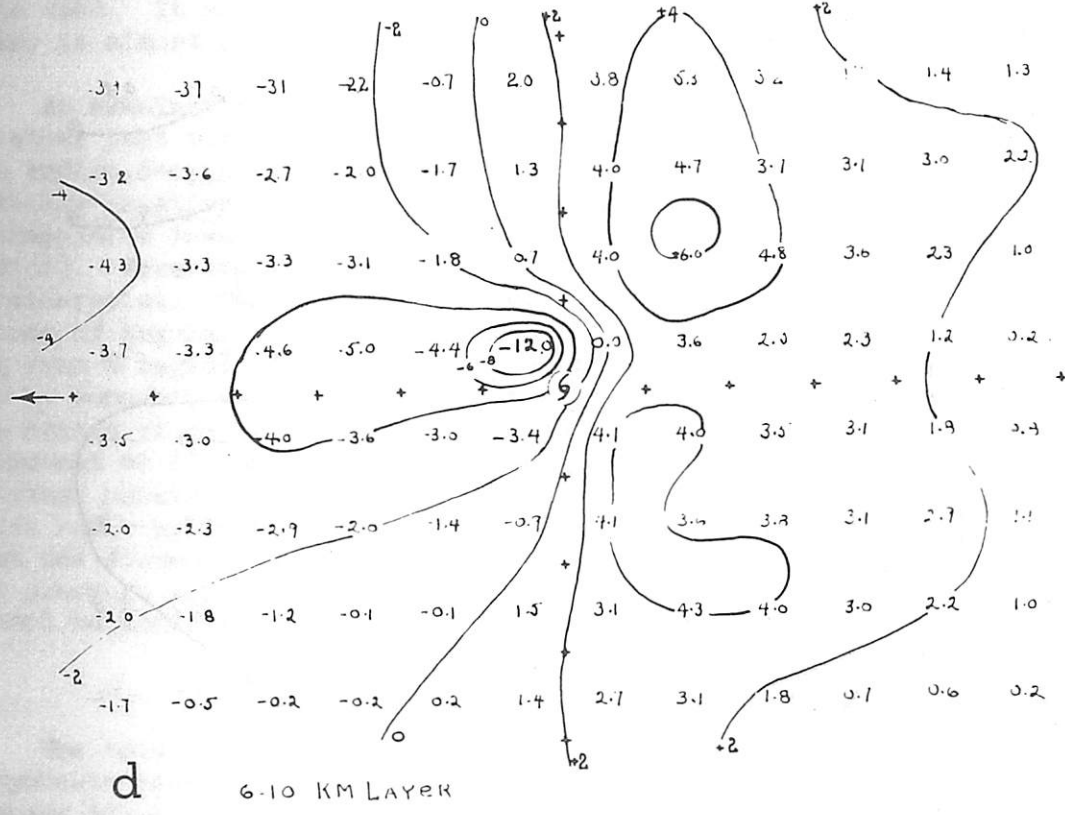


Figure 6. - Radial motion (speed in m.p.s.). Negative values indicate outflow.



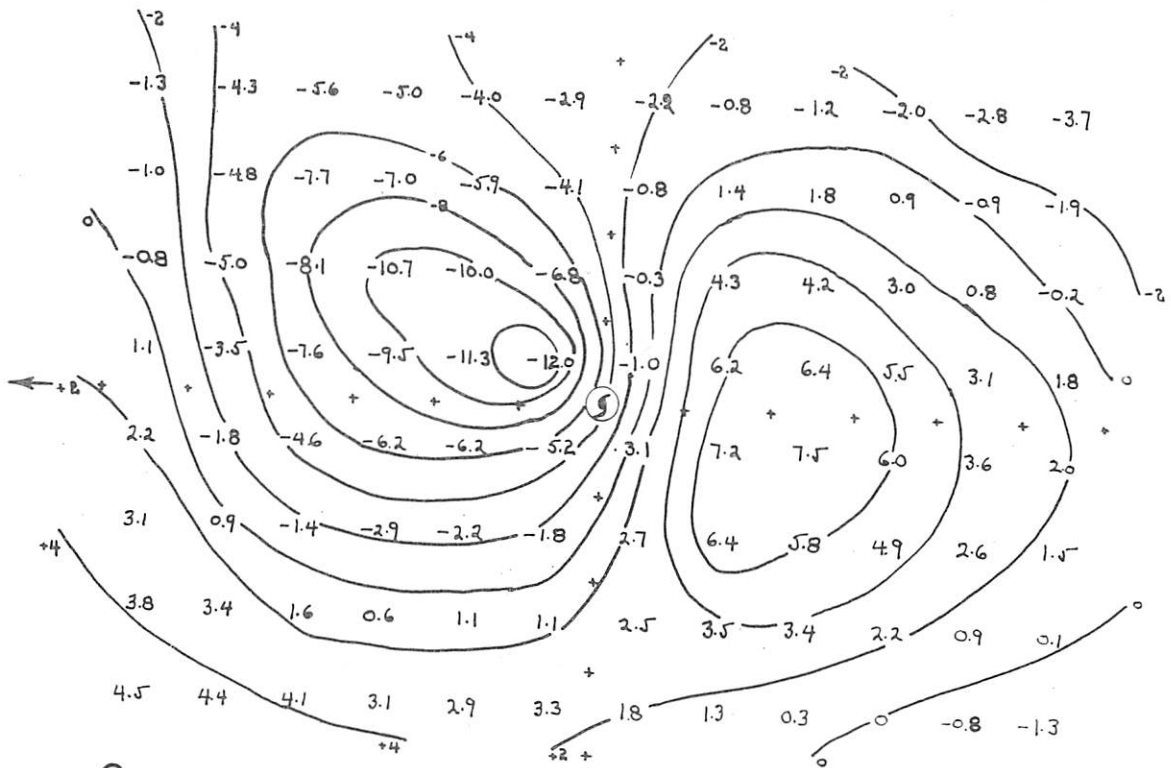
SCALE 2 4  
°LAT

SCALE 2 4  
°LAT



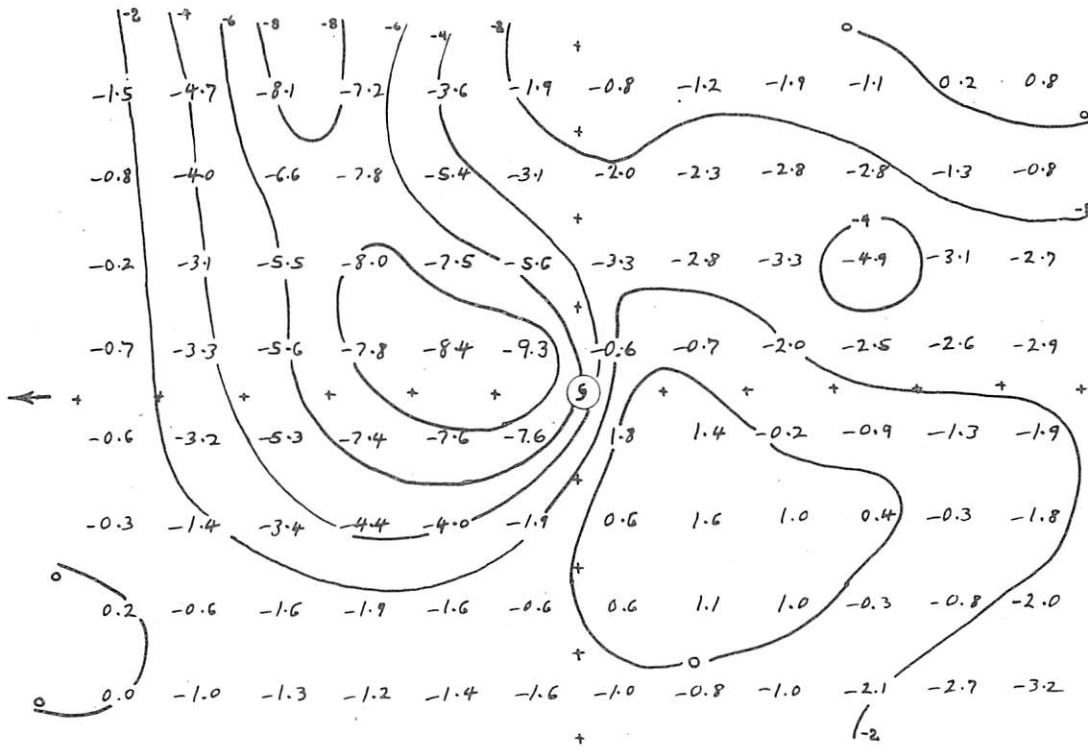
ate outflow.

Figure 6. - Radial motion (continued)



e 10 TO 12.5 KM LAYER

SCALE 4 °LAT



f 12.5 TO 16 KM LAYER

Figure 6. - Radial motion (continued)

Which of the two profiles is correct is questionable, although at first glance that of Hughes appears more reasonable. However, this may not necessarily be so. As stated previously there are some indications that the angle of inflow decreases as one approaches the center of the storm and the wind velocity increases, but whether or not this decrease is large enough to cause the radial component to decrease is not clear. The radial velocity must obviously begin to decrease at some finite distance from the center of the hurricane. The present data would seem to indicate that this decrease begins somewhere within the  $2^\circ$  to  $3^\circ$  ring, although intuitively one would expect it to occur much closer in. Further work on the true wind-pressure-centrifugal force relationship would seem to be indicated before the true radial velocity profile can be established.

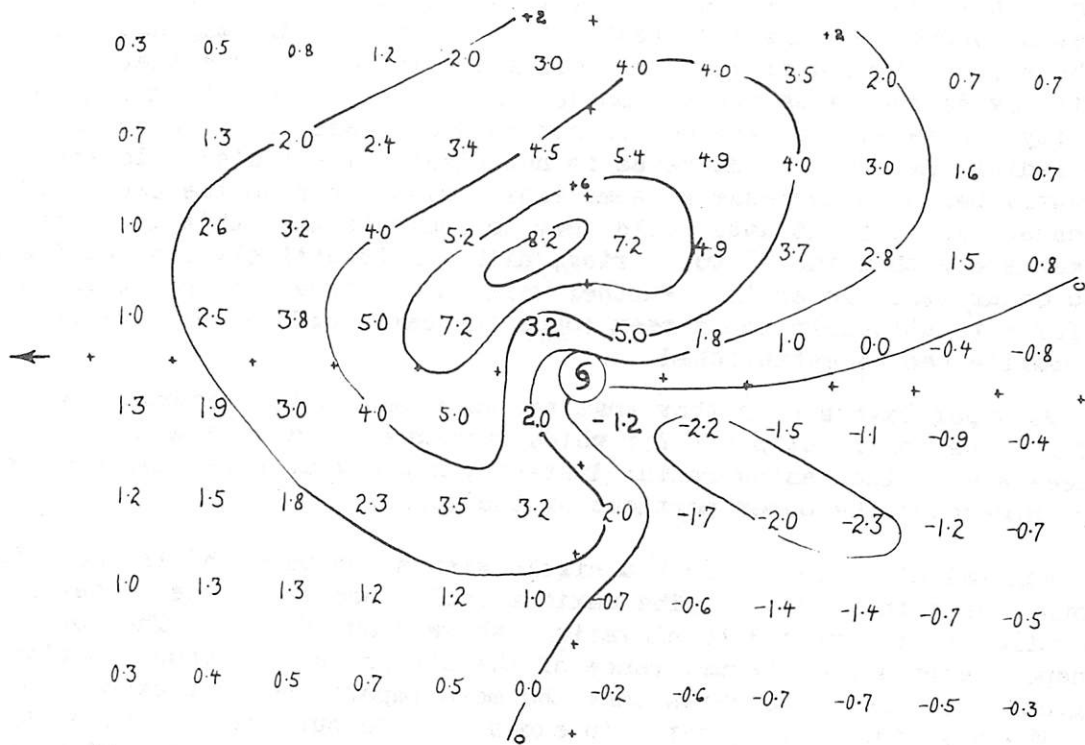
The two upper layers both show that the maximum outflow occurs at a radius of  $1^\circ$  (the innermost point for which averages could be compiled) and this decreases with increasing radial distance, rapidly at first and then more gradually throughout the outer portions of the storm.

The mean radial motion through a circle with a radius of  $3^\circ$  is shown for the various layers in figure 9. The maximum inflow occurs in the lowest 1 km. and net outflow is restricted to elevations above about 8.5 km. The total mass transport across the circumference of the circle is also shown in figure 9. Integration of the curve shows that the mass import and mass export do not balance. The mass inflow is greatly in excess of the outflow. In order to balance, a mean upward motion of about 32 cm. sec.<sup>-1</sup> would be required over the  $3^\circ$  circle at 16 km., the top of the upper layer. The actual average is about 29 cm. sec.<sup>-1</sup>, (fig. 15f) which is as close as can be expected from the data used. It may be of significance that the mass import through the lowest 1 km. is almost exactly balanced by the mass export above 10 km.

An examination of the inner portions of the 1-3-km. radial profile (fig. 8) shows that the decrease from the maximum inflow at  $3^\circ$  radius continues as the radius decreases and that at  $1^\circ$  the indicated mean radial component is actually negative. This value is naturally suspect, since the data for  $1^\circ$  are extrapolated inward from the last point for which data were tabulated ( $1.4^\circ$  radius). However, it may be real and should not be dismissed without some consideration. The air rising from the lower layers possesses a very large amount of angular momentum, which should be conserved. Since the air is rising from a region of intense pressure gradient to an area where the gradient may be somewhat weaker, some of the rising air may be flung outward, due to the excess of centrifugal force over the pressure gradient. The mean radial component at  $1^\circ$  was also negative in the 3-6 and 6-10-km. layers. It is surprising, however, that such an outflow (if it exists) could be detected by the gross scale used in tabulating the data, and for this reason, plus the fact that the foregoing argument concerning the excess of centrifugal force over the pressure gradient is of doubtful validity, the existence of such outflow cannot be accepted without further investigation.

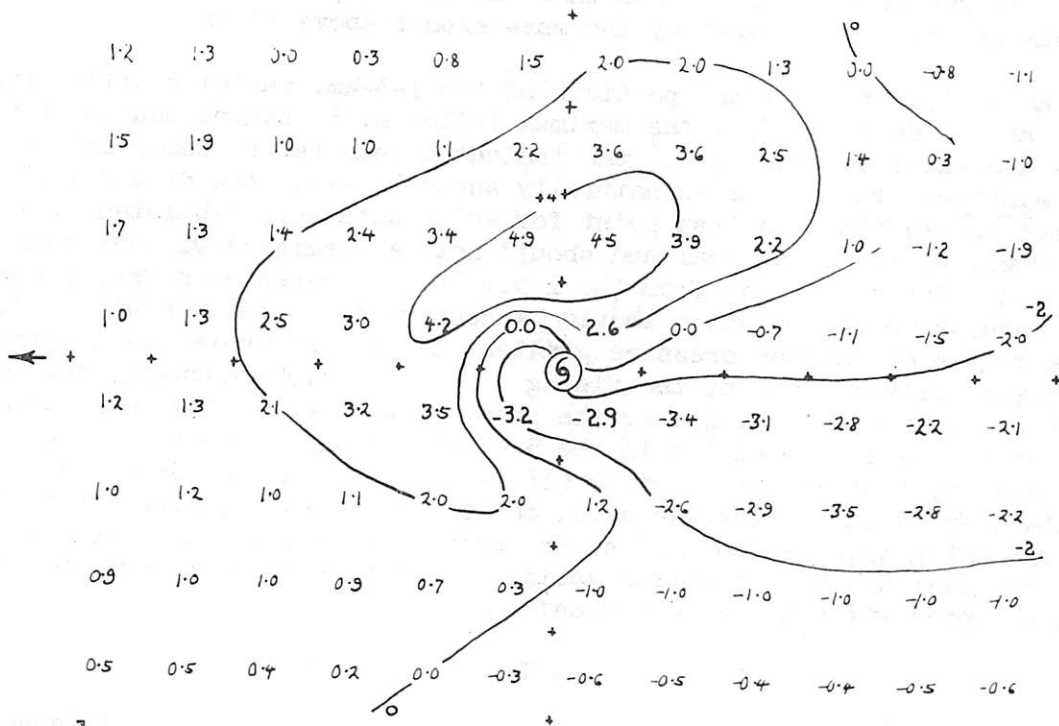
## 8. THE TOTAL AND RELATIVE WIND FIELDS

The total wind fields, which comprise the sum of the radial and tangential components plus the motion of the storm, for the several layers are shown in figures 10a-f. The relative wind fields, from which the motion of the storm has been removed, are shown in figures 11a-f. They represent essentially the circulation about a stationary storm. Both sets of charts are virtually self-explanatory.



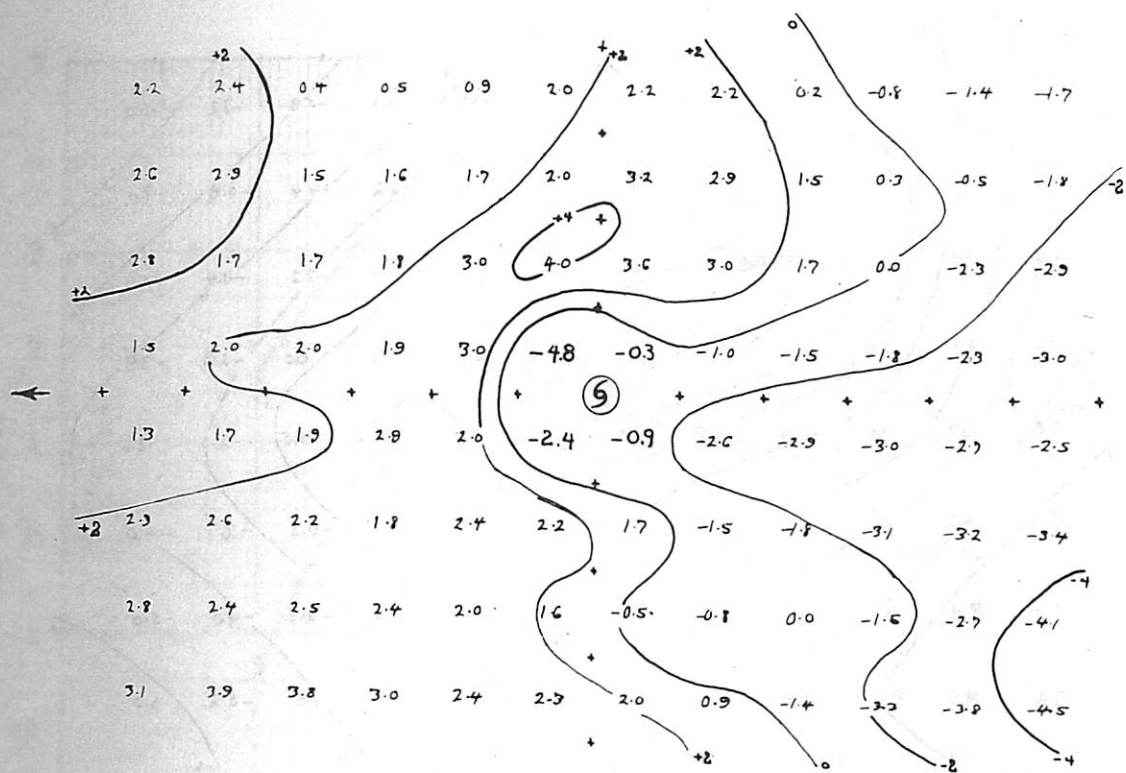
a 0-1 km layer

Scale 2° Lat



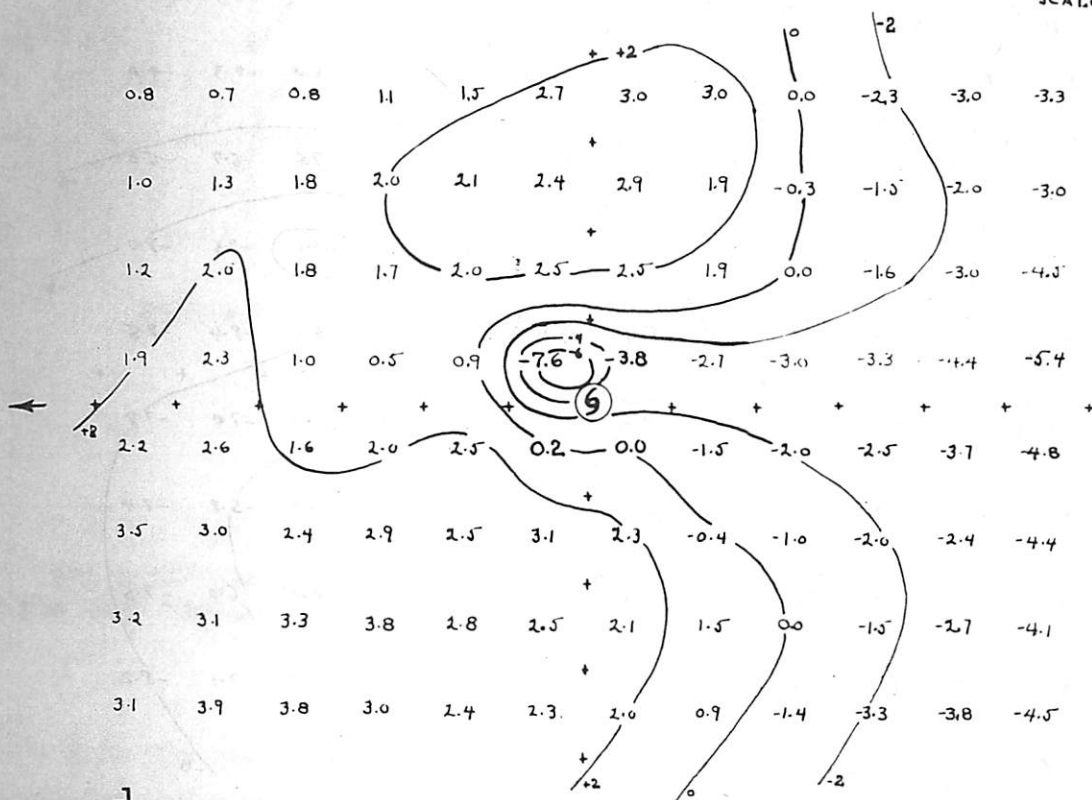
b 1-3 km layer

Figure 7. - Radial motion (speed in m.p.s.) relative to center of storm. Negative values indicate outflow.



c 3-6 km layer

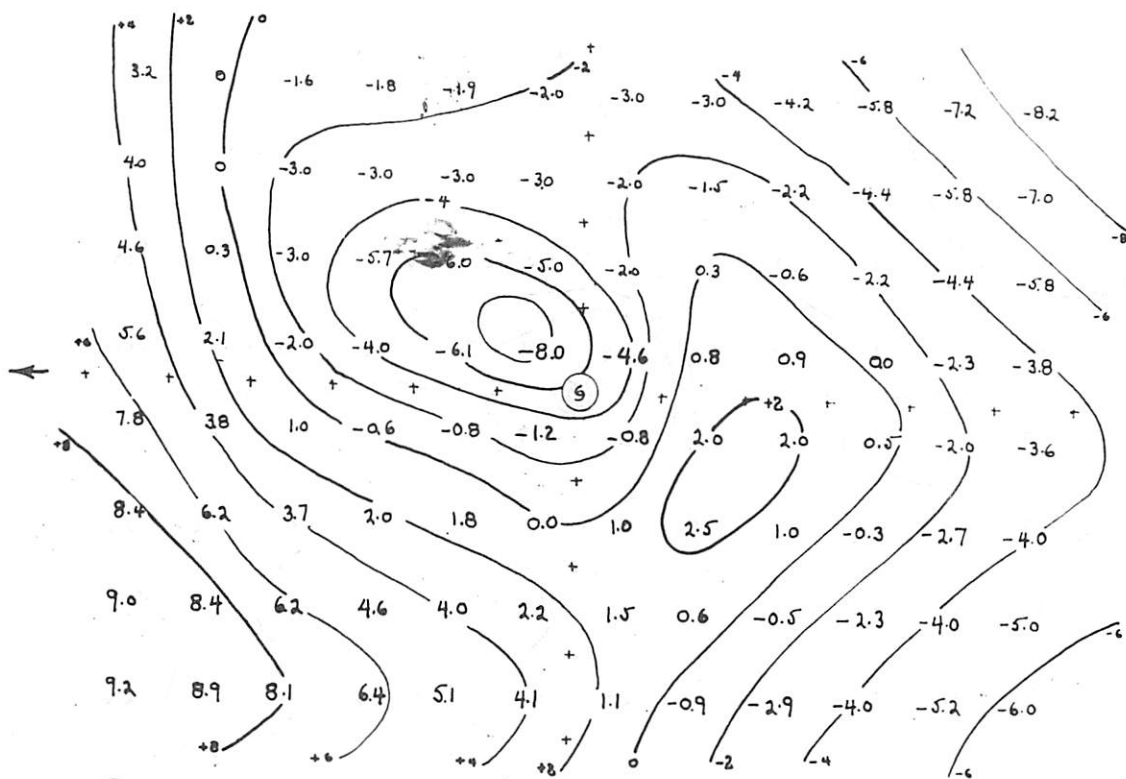
SCALE 0 2 4  
°LAT



d 6-10 km

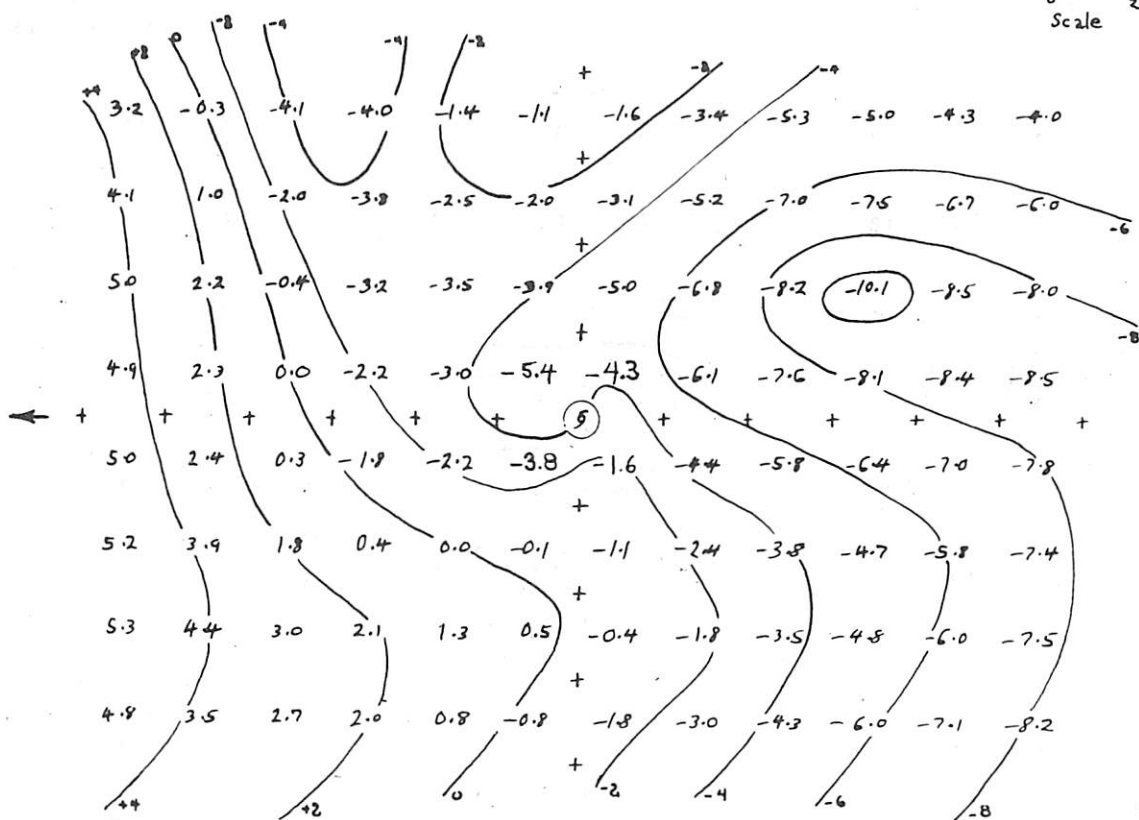
Figure 7. - Radial motion relative to center (continued)

m.



10 TO 12.5 KM

Scale 0 2 4  
°Lat



12.5 TO 16 KM

Figure 7. - Radial motion relative to center (continued)

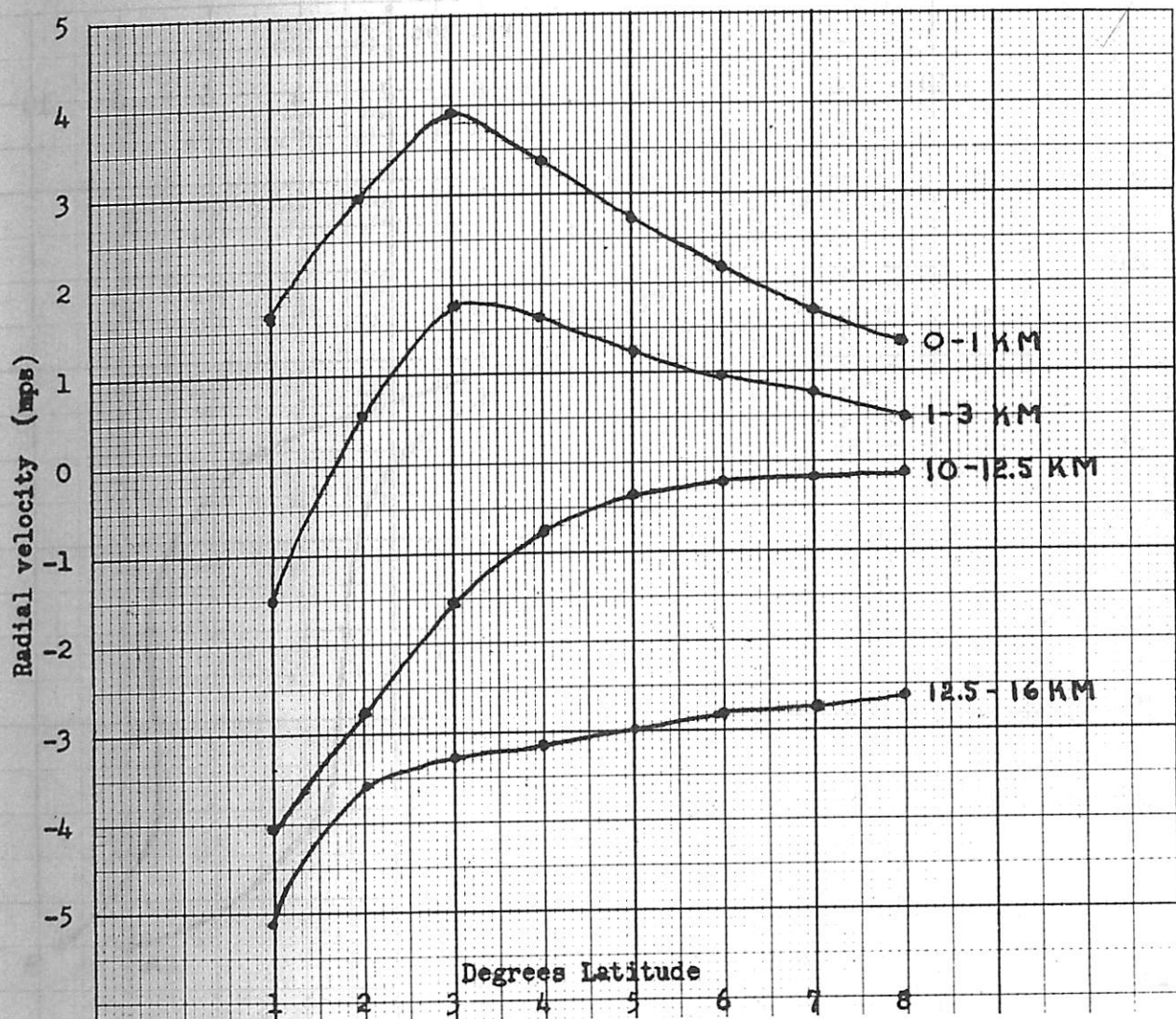


Figure 8. - Radial velocity profile for various layers.

#### 9. THE MEAN VORTICITY

The mean relative vorticity was calculated from the tangential components in the same manner used by E. Jordan [2] who used the formula

$$\zeta = 2 (r_0 v_0 - rv) / (r_0^2 - r^2) \quad (4)$$

where  $\zeta$  is the relative vorticity,  $r_0$  and  $r$  are the radii and  $v_0$  and  $v$  are the tangential velocities of the inner and outer portions of a given ring. Computations were made for rings  $1^\circ$  of latitude in width, beginning at  $1^\circ$  and extending out to  $8^\circ$ . The results are shown in figure 12.

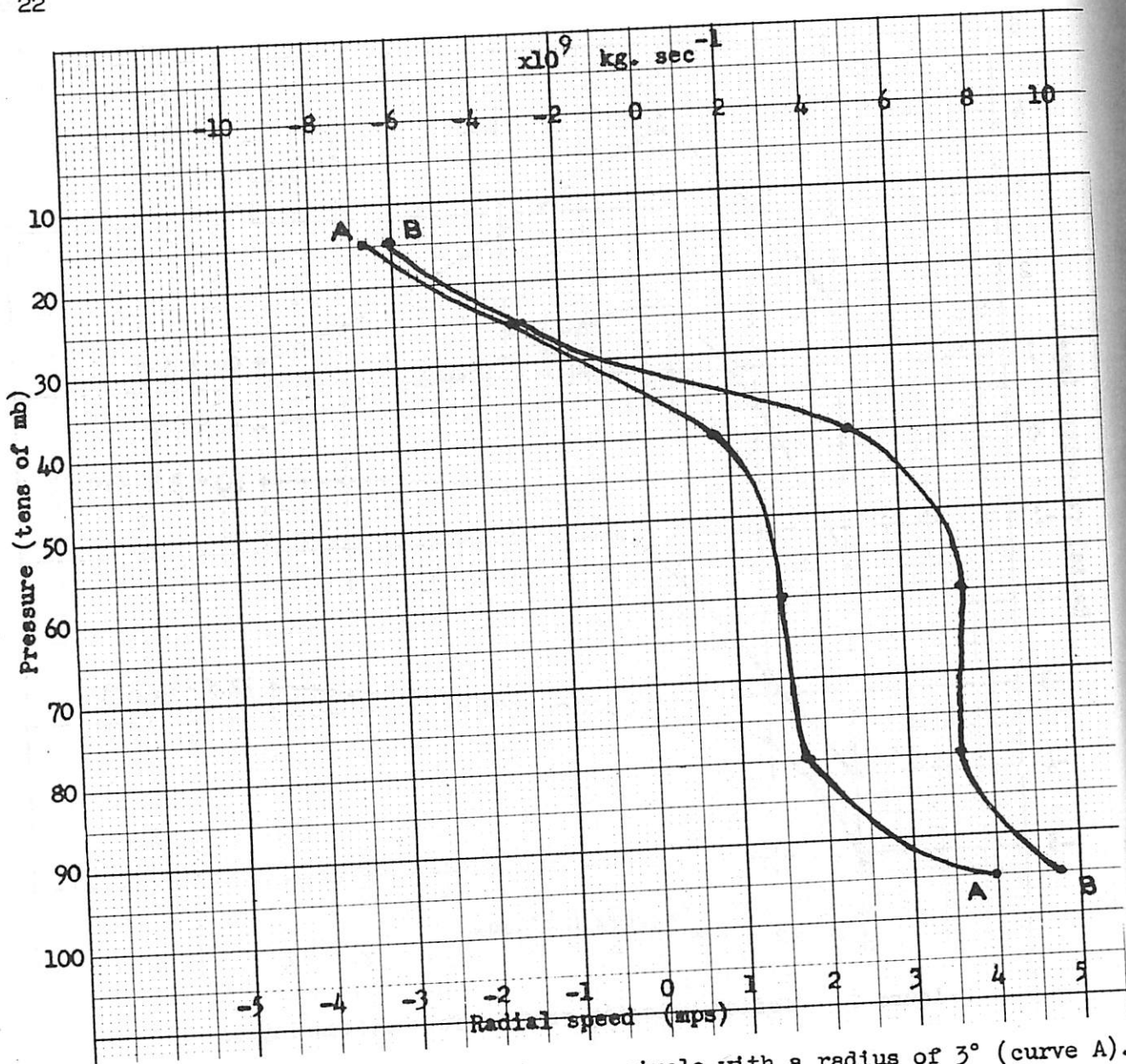


Figure 9. - Mean radial motion across a circle with a radius of  $3^\circ$  (curve A).  
Total mass transport across the same circle (curve B).

The relative vorticity ranged from  $9.7 \times 10^{-5} \text{ sec.}^{-1}$  for the two lower layers in the  $1^\circ$ - $2^\circ$  ring to  $-2.0 \times 10^{-5} \text{ sec.}^{-1}$  for the highest layer in the  $4^\circ$ - $5^\circ$  ring. For the inner ring the relative vorticity was almost constant up to about 600 mb, above which it dropped off rapidly, becoming negative near 200 mb. Laterally the relative vorticity was negative for all levels outside the  $4^\circ$ - $5^\circ$  ring.

A comparison with the work of Hughes [1] shows excellent agreement between his values, based on reconnaissance aircraft wind data taken near 1000 feet, and those of the present data for the 0-1-km. layer. Agreement for the upper layers with the work of E. Jordan [2] is not as good, the main differences

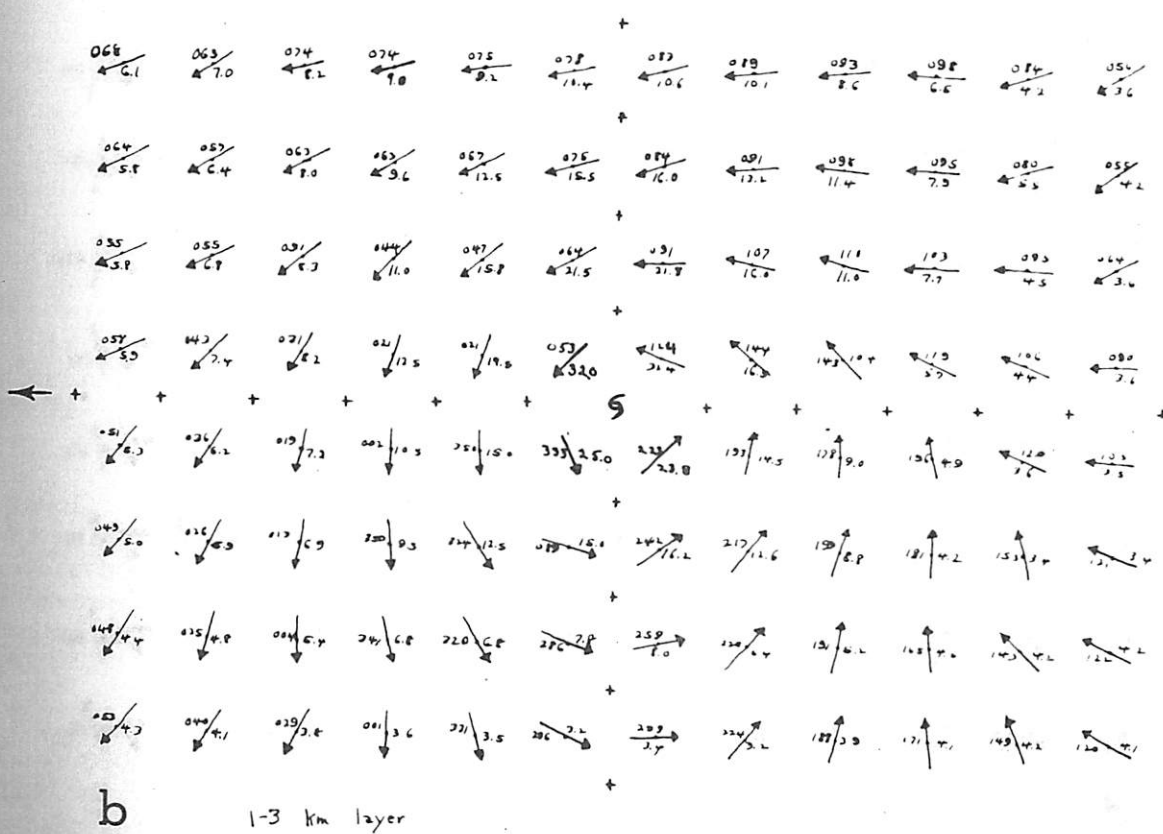
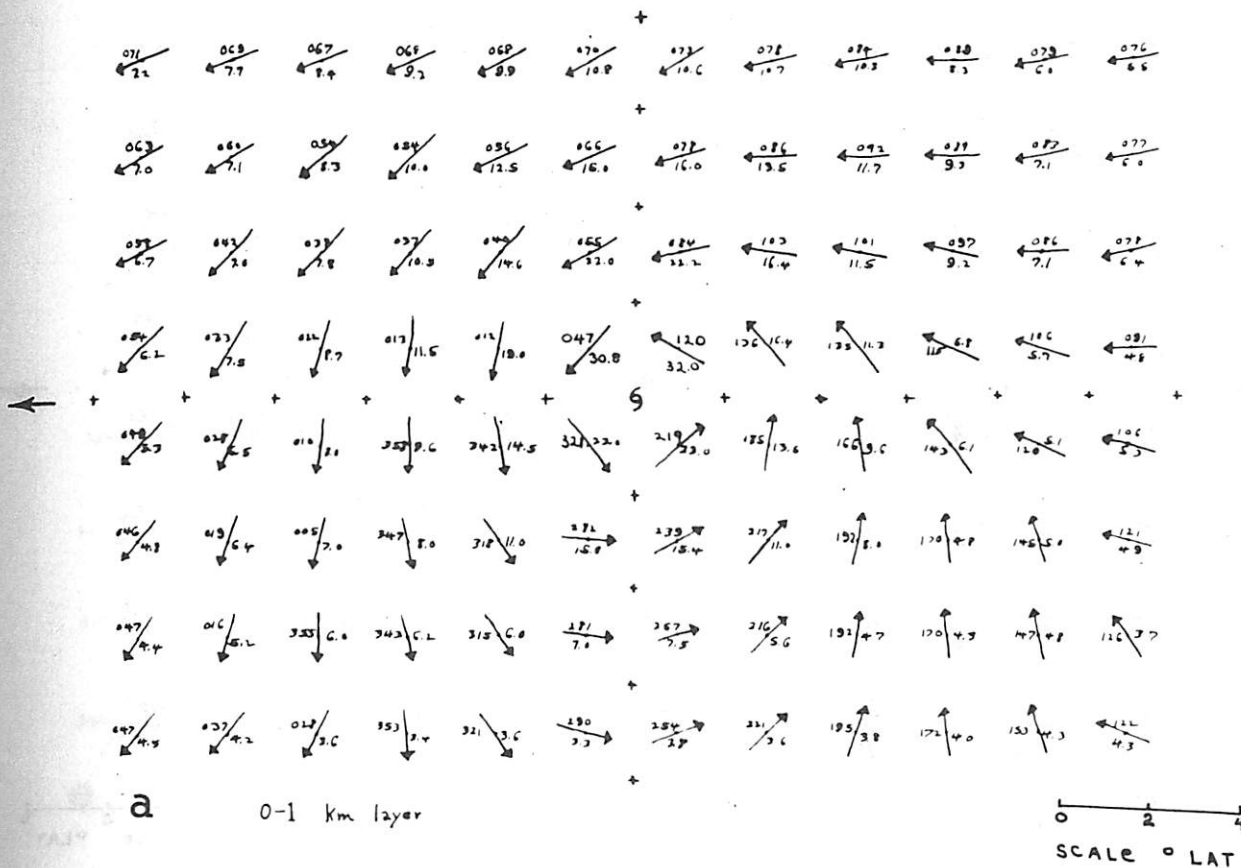
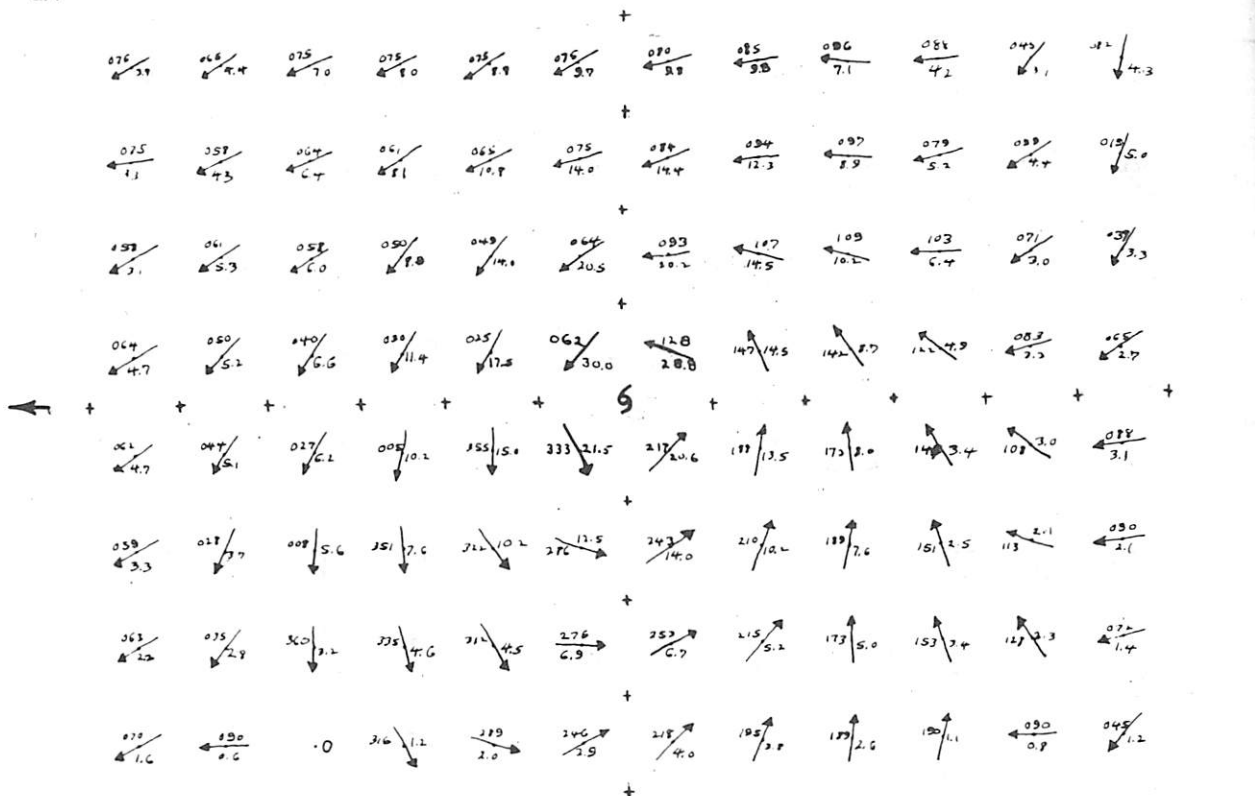


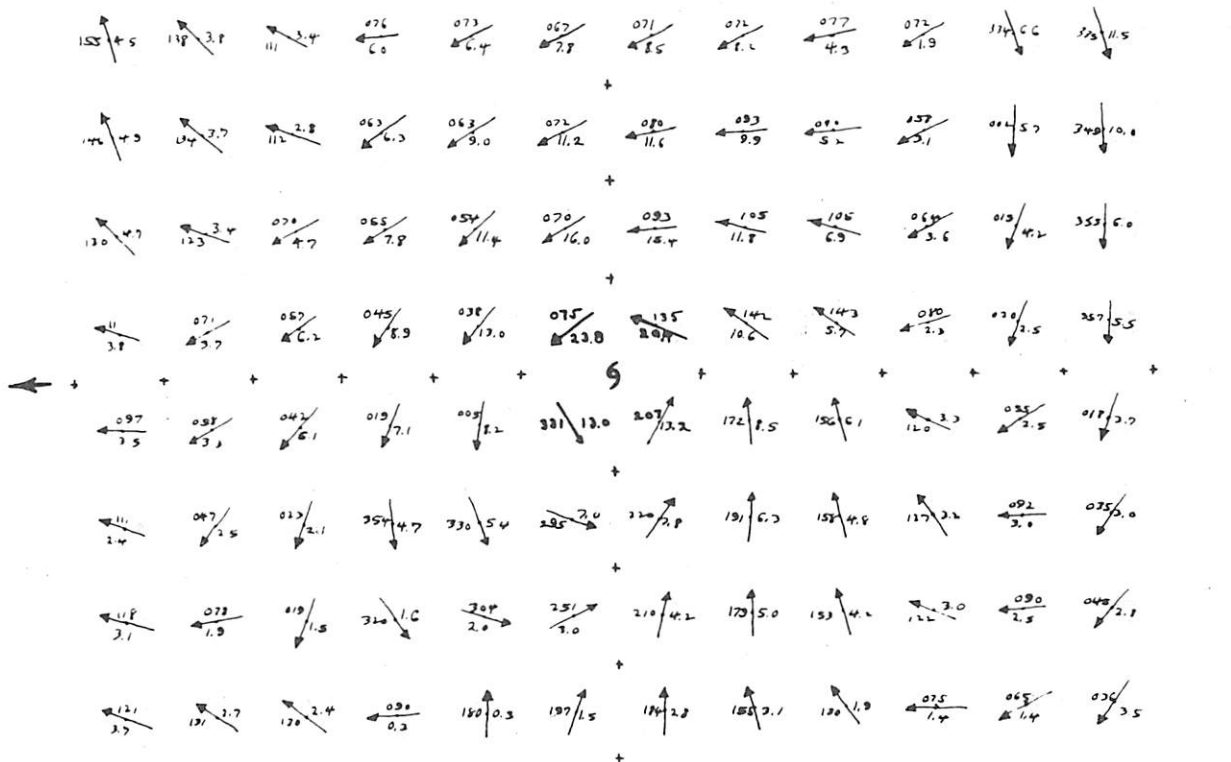
Figure 10. - Mean wind field. Speed in m.p.s.

er  
the  
it  
near  
side  
between  
et,  
upper  
es



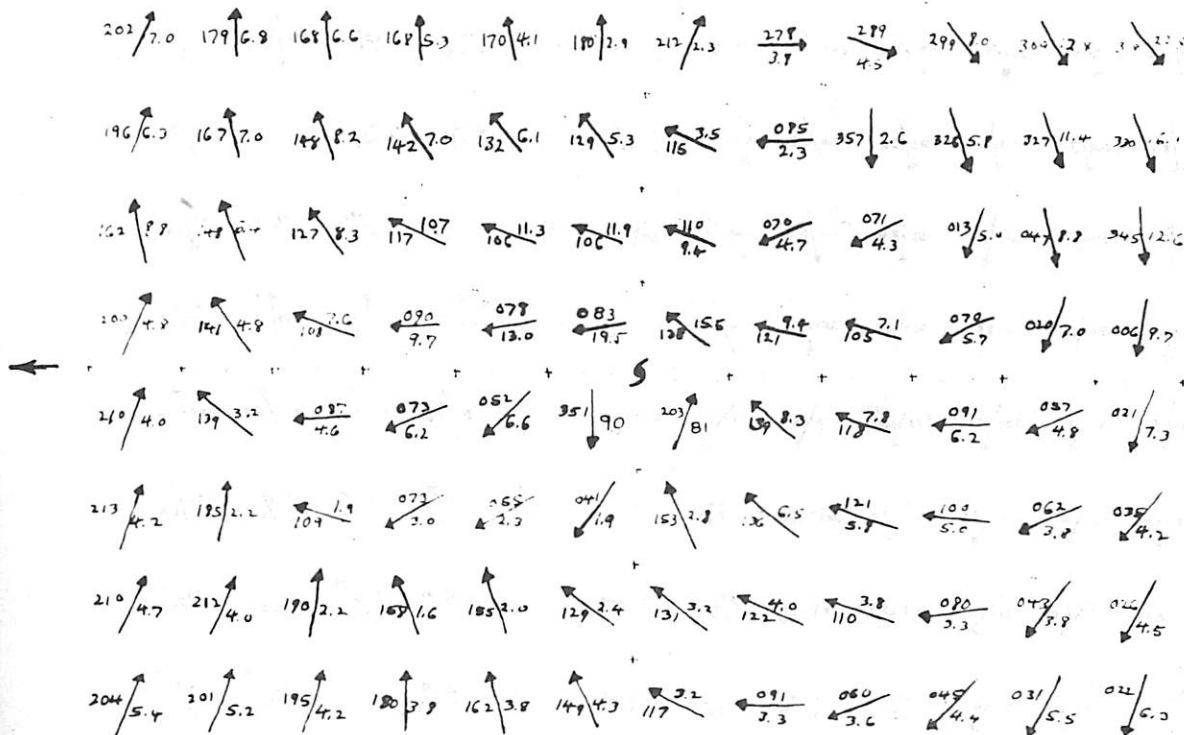
C 3-6 km layer

0 2 4  
SCALE °LAT



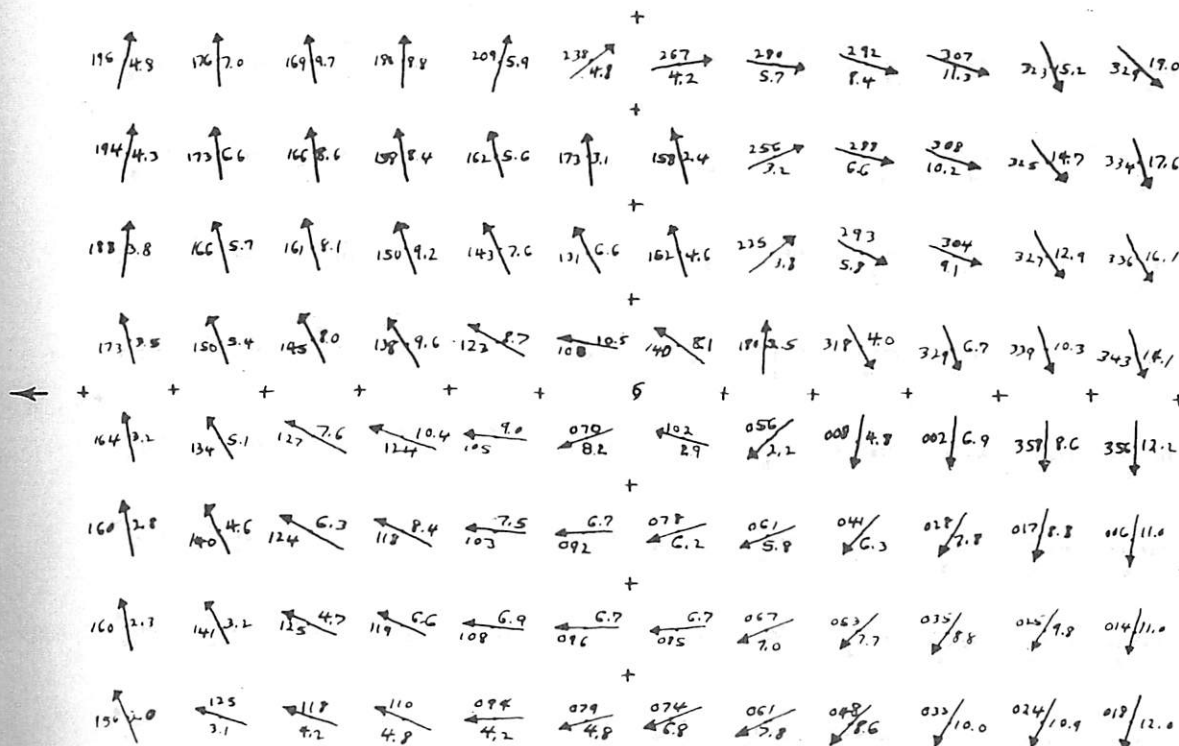
d 6-10 km layer

Figure 10. - Mean wind field (continued)



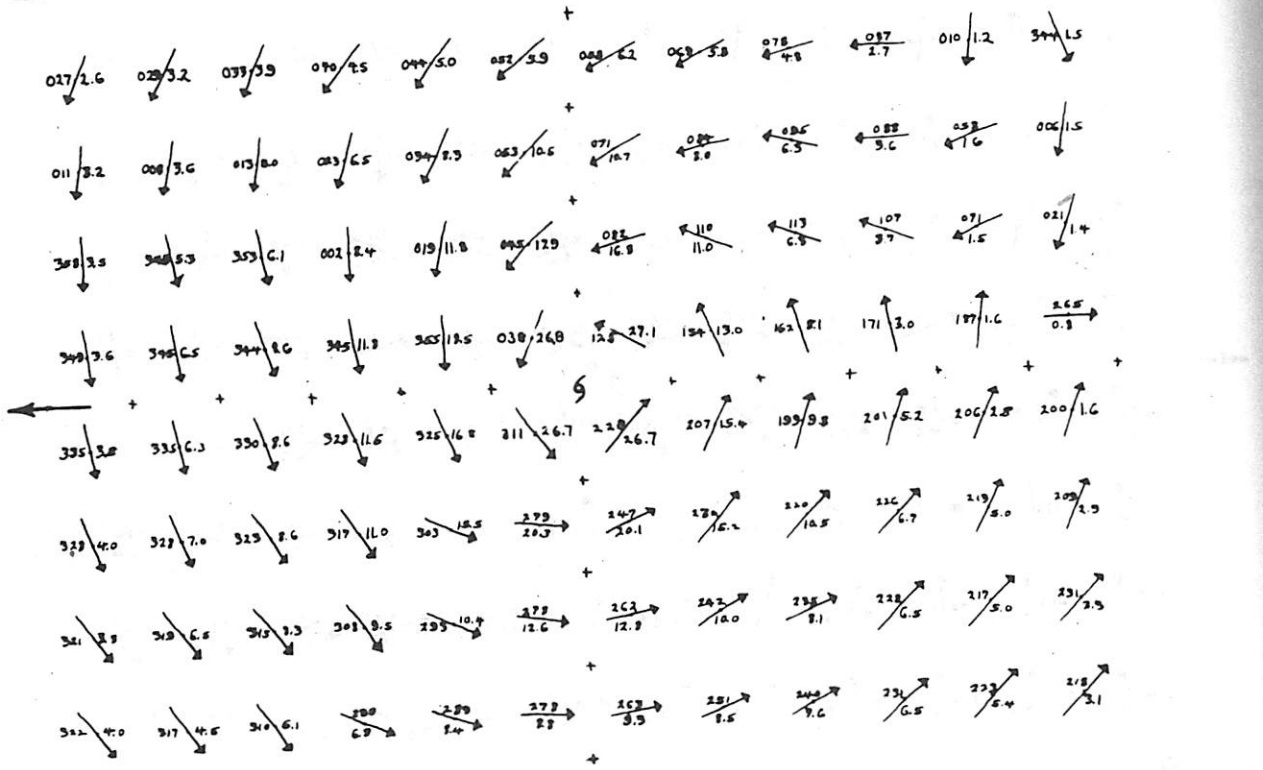
e 10 TO 12.5 KM LAYER

SCALE 2 4 °LAT



f 12.5 TO 16 KM LAYER

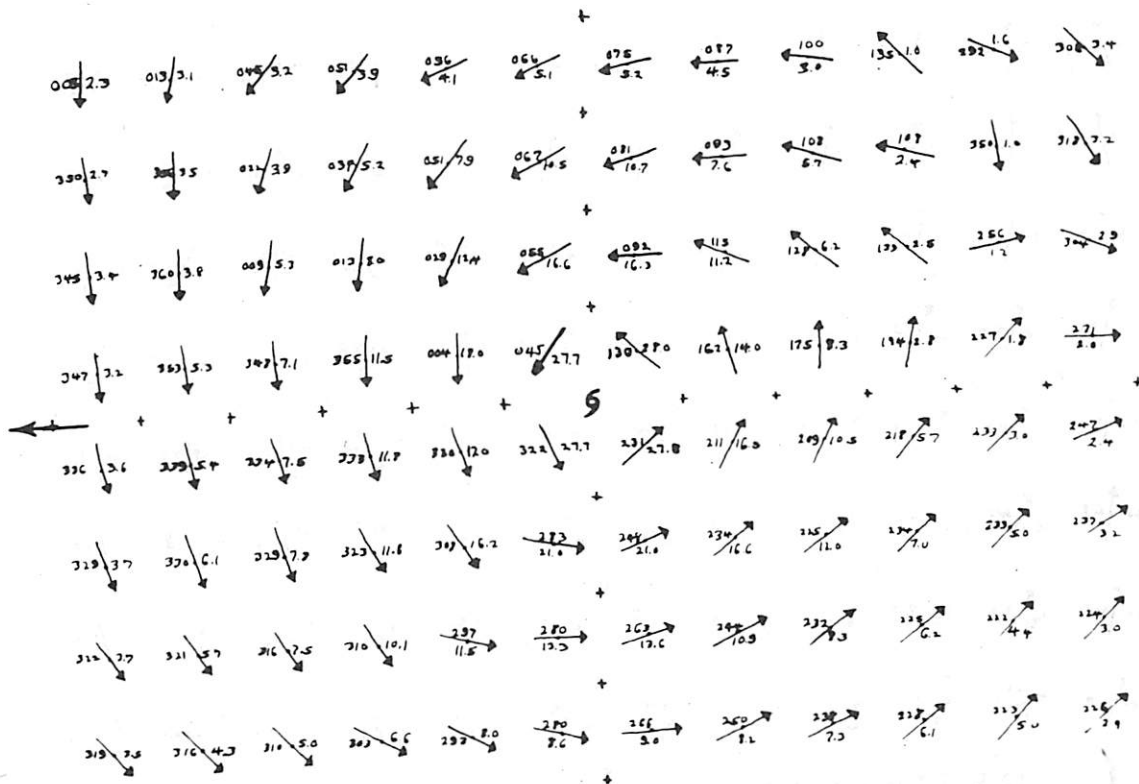
Figure 10. - Mean wind field (continued)



a

0-1 km layer

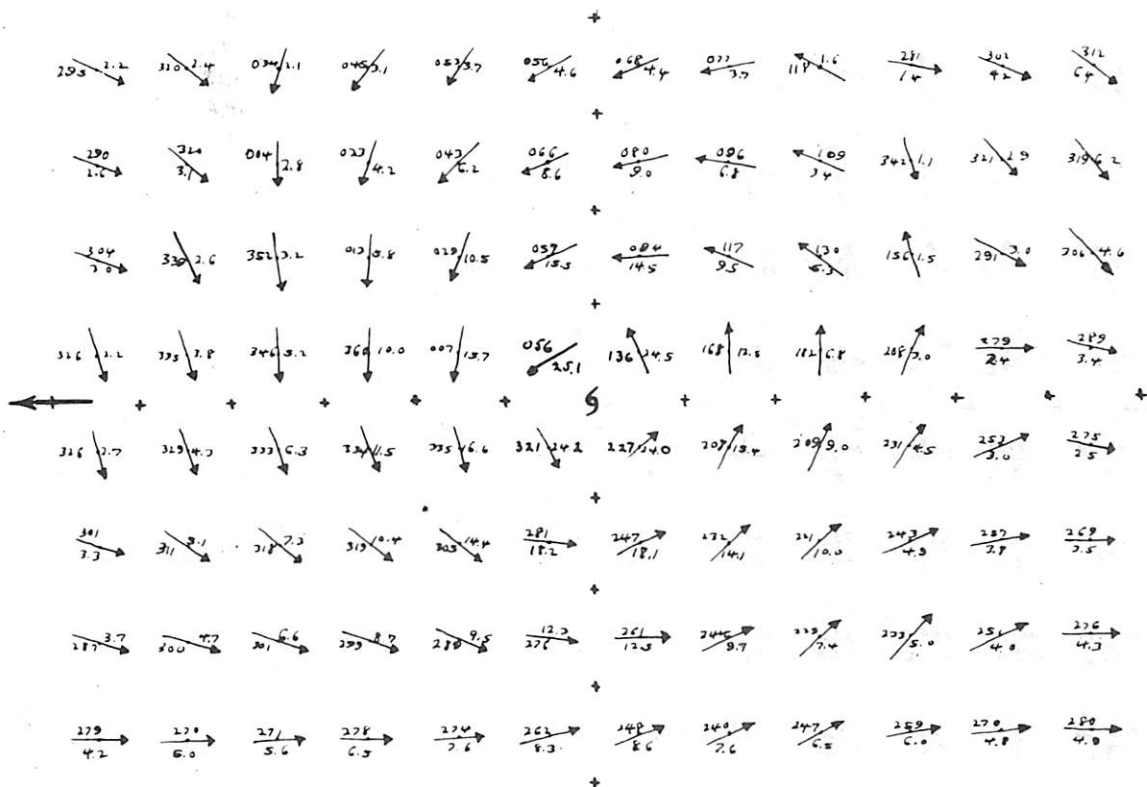
SCALE = LAT



b

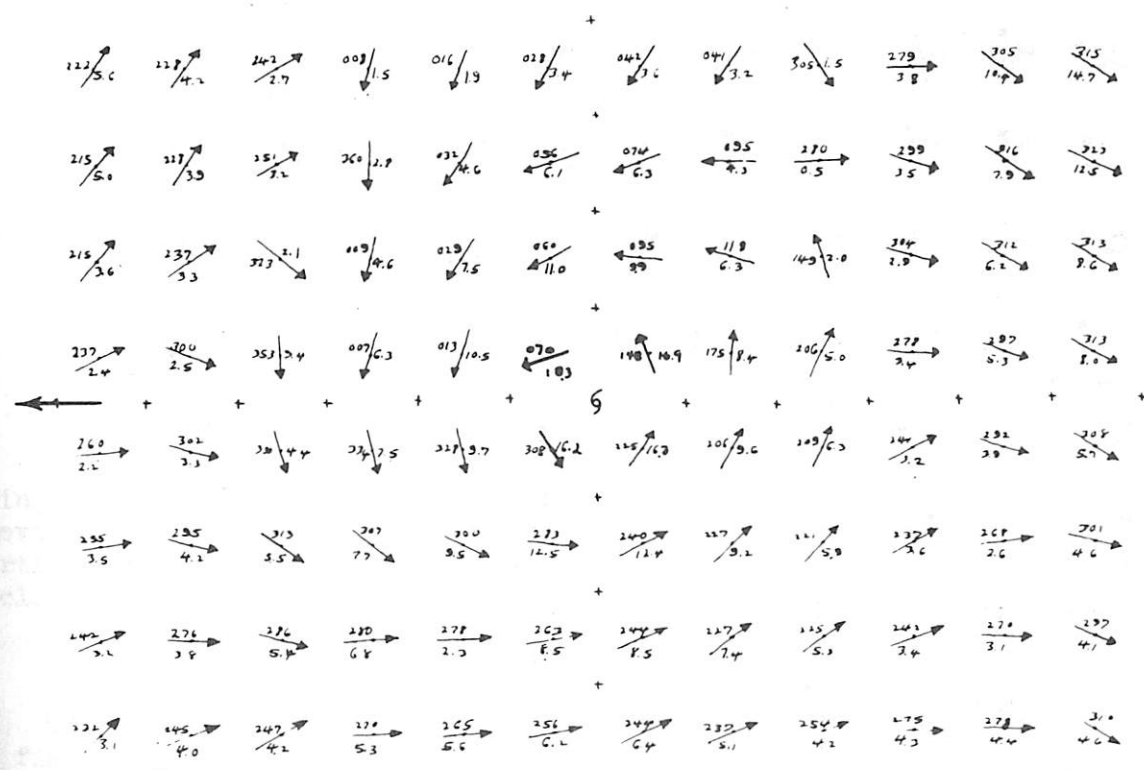
1-3 km layer

Figure 11. - Mean wind field with motion of storm removed. Speed in m.p.s.



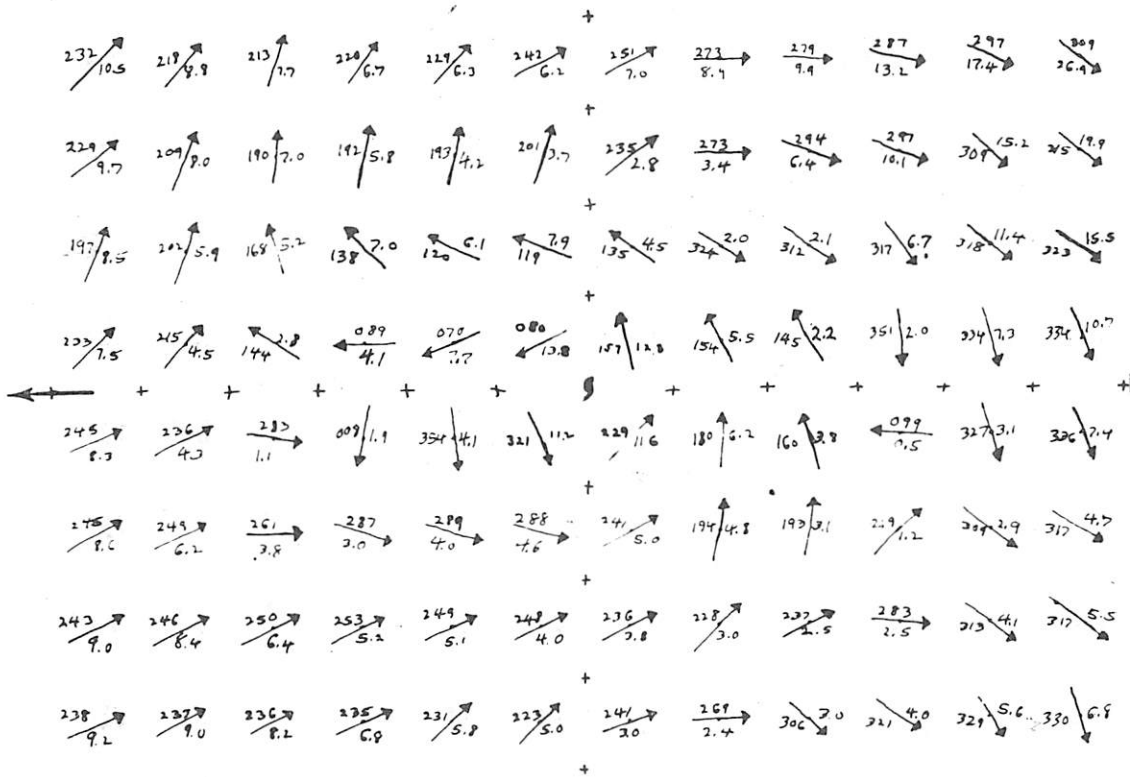
C 3-6 km layer

0 2 4  
SCALE ° LAT



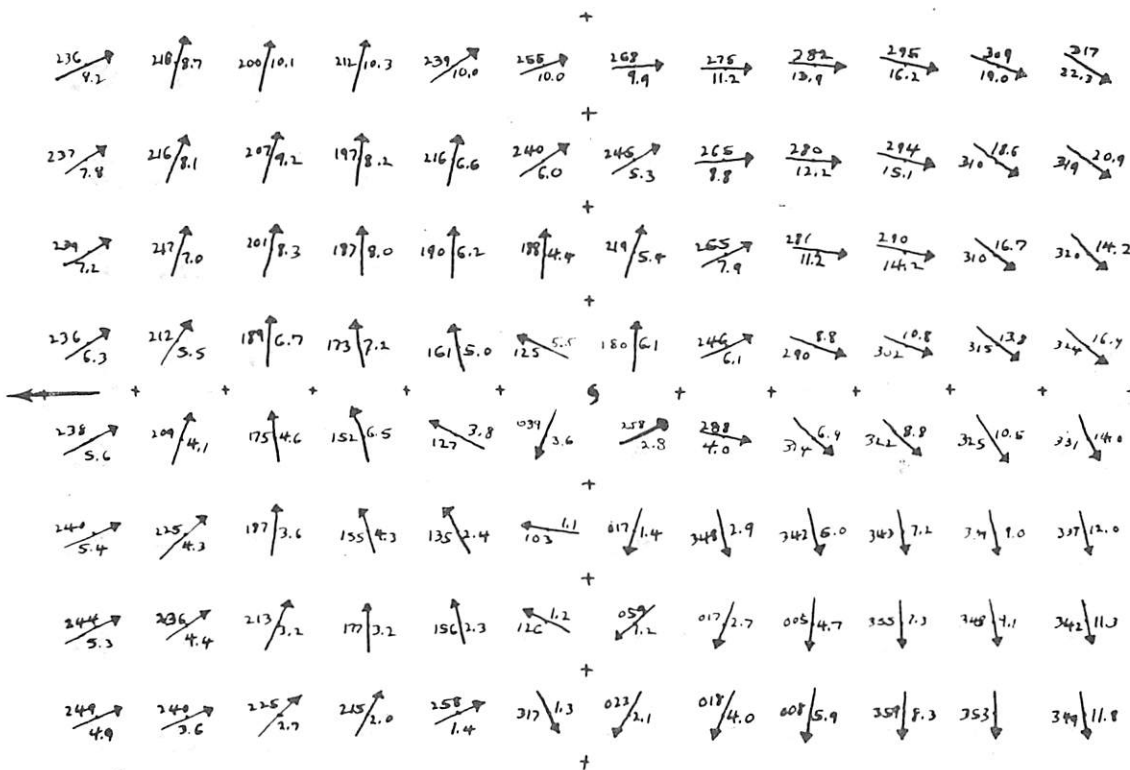
d 6-10 km layer

Figure 11. - Mean wind field (minus storm motion) (continued)



e 10 TO 12.5 KM LAYER

0 2 4  
SCALE °LAT



f 12.5 TO 16 KM LAYER

Figure 11. - Mean wind field (minus storm motion) (continued)

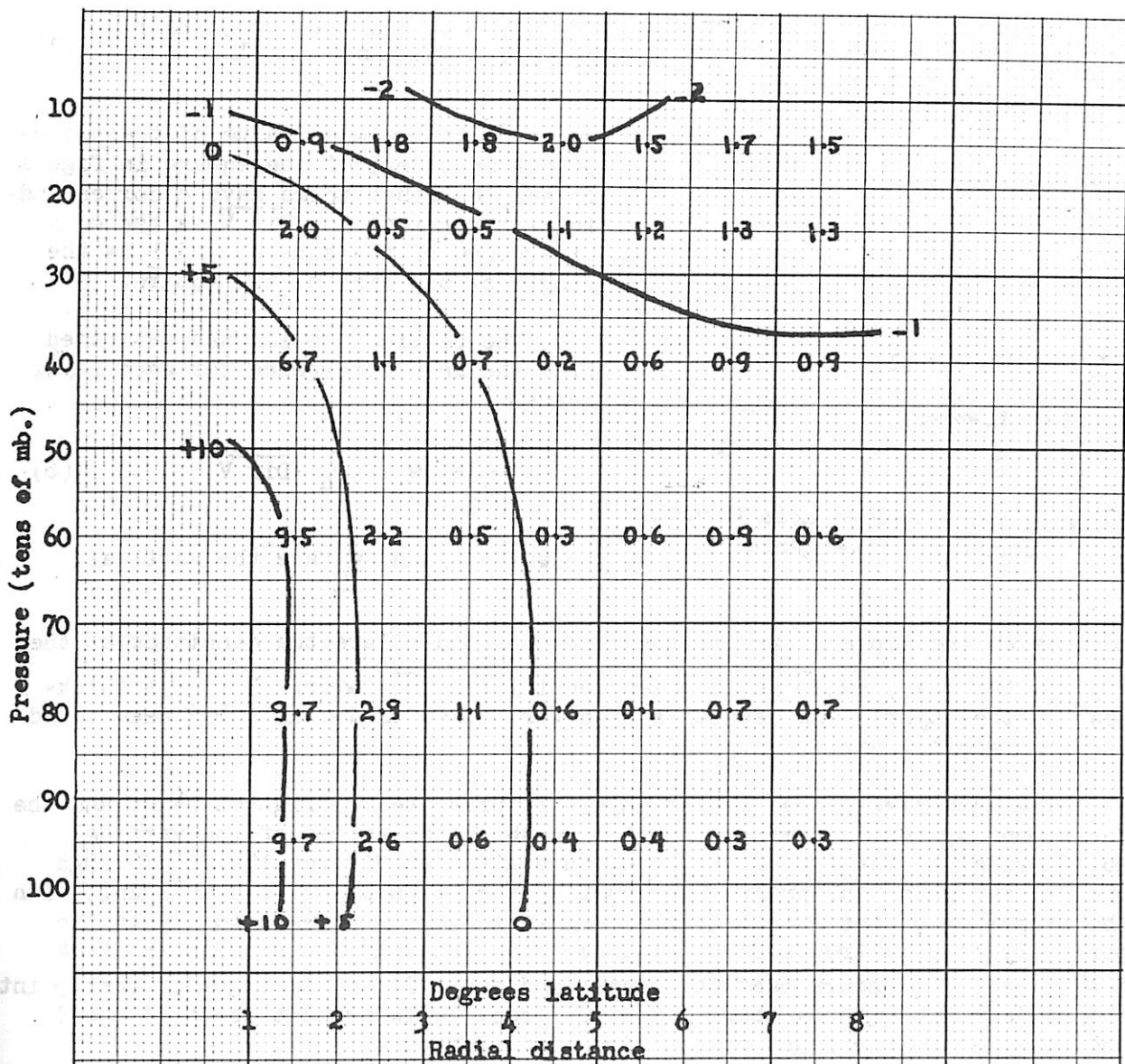


Figure 12. - Cross section of relative vorticity ( $10^{-5}$  sec. $^{-1}$ ).

being that the present data show that the positive vorticity extends to higher elevations and also fail to substantiate her conclusion that negative absolute vorticity may exist within the upper troposphere in the vicinity of a tropical cyclone.

#### 10. DIVERGENCE AND VERTICAL MOTION

The mean divergence was computed over  $2^\circ$  squares from the mean wind data of figures 10a-f. The square shown in figure 13 and the following relationship [6] were used:

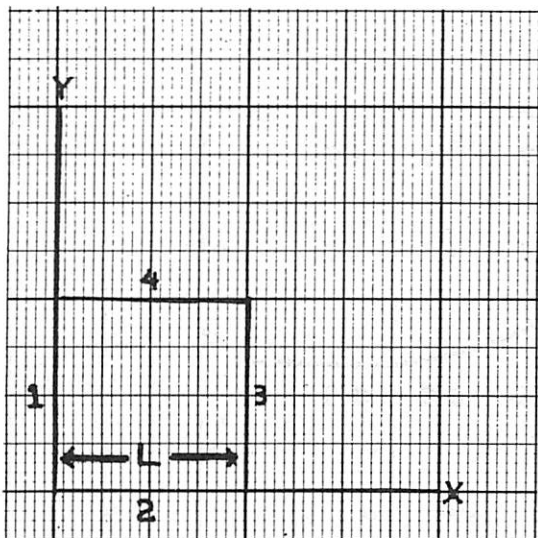


Figure 13. - Square area used in computing divergence.

$$\overline{\text{Div } V} = \frac{(u_3 - u_1) + (v_4 - v_2)}{L} \quad (5)$$

where  $u_3$  is the mean value of the  $u$  component on side 3 of the square in figure 13 and the other terms have a corresponding interpretation.  $\overline{\text{Div } V}$  is the mean divergence of the square, and  $L$  is the length of one side of the square.

The vertical motion was evaluated from the mean divergence for each layer using

$$w_h = \frac{\rho_o}{\rho_h} w_o - \bar{\rho} \overline{\text{Div } V} \quad (6)$$

in which  $w_h$  and  $w_o$  are the vertical

motions at the top and base of the layer,  $\rho_h$  and  $\rho_o$  are the densities at the top and the base, and  $\bar{\rho}$  is the mean density for the layer.  $h$  is the thickness of the layer. The densities used were based on Jordan's [3] mean sounding for tropical air.

The mean divergence for the layers is presented in figures 14a-f and the corresponding vertical motion charts, in which the values of the vertical motion refer to the top of the layer, are given in figures 15a-f. Through the 0-1-km. layer the entire rear half of the circulation is convergent, with the exception of the extreme right rear sector which appears to lie in the periphery of a subtropical anticyclone. The maximum convergence, about  $-4 \times 10^{-5} \text{ sec.}^{-1}$ , occurs near the center and about  $2^\circ$  to the right of that point. The maximum divergence, about  $1.4 \times 10^{-5} \text{ sec.}^{-1}$ , is present about  $4^\circ$  ahead and about  $2^\circ$  to the right of the direction of motion.

The relative positions of the maximum convergence and divergence agree substantially with the computations of Hughes [1], although the convergent area is larger for the present data, the center of maximum divergence is farther out than Hughes found it to be, and the values of the maximum convergence are only about one-third those presented by Hughes. Two reasons may be responsible for these differences. First, the value of divergence depends to some extent upon the scale over which it is computed [5]. The values of figure 14a were obtained by averaging over squares of  $2^\circ$  latitude, whereas Hughes used a smaller scale for his computations. Second, the radial velocity of Hughes showed increasing values of the radial component to within  $0.5^\circ$  of the center, while the present data indicate a decrease inside  $3^\circ$ . Both these factors serve to make the convergence near the center less for the present data than for the sample Hughes used.

Through the 1-3-km. layer, a small divergent area has appeared just to the rear of the center of the storm, and the value of the convergence over

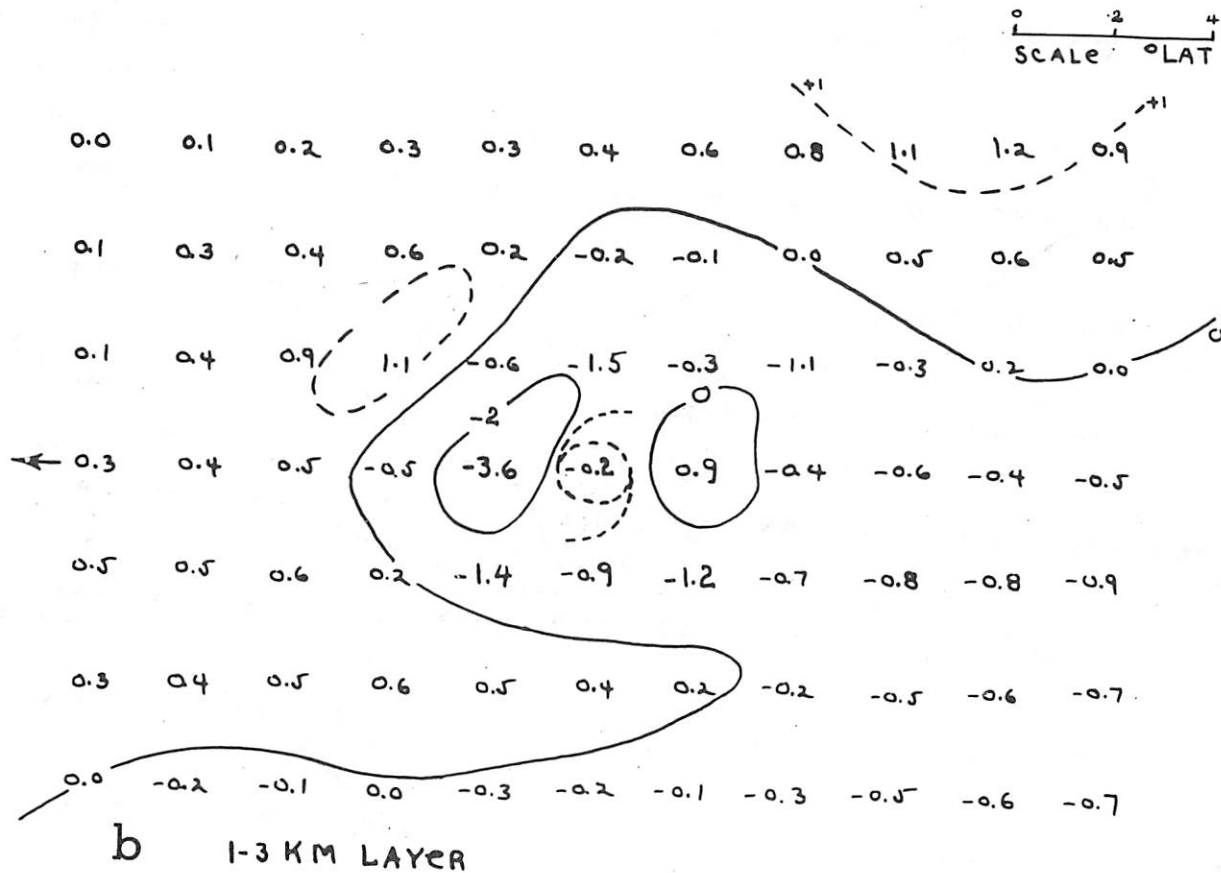
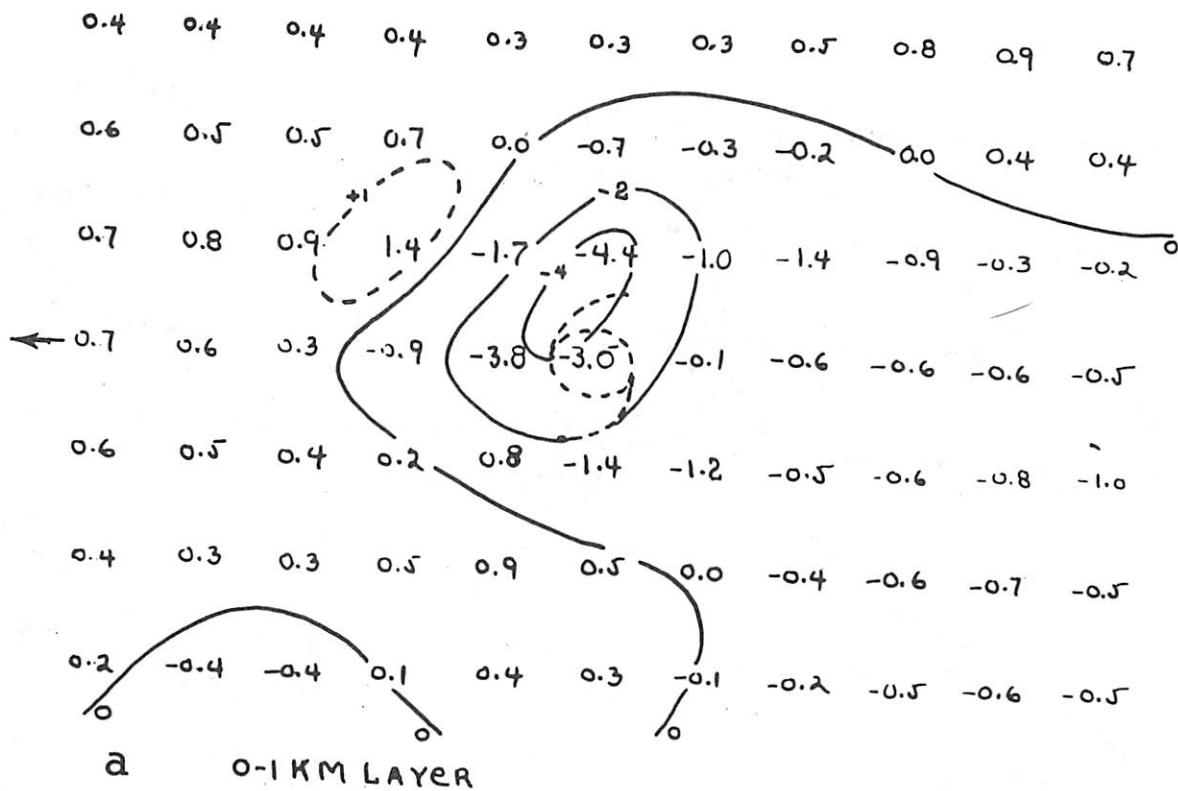
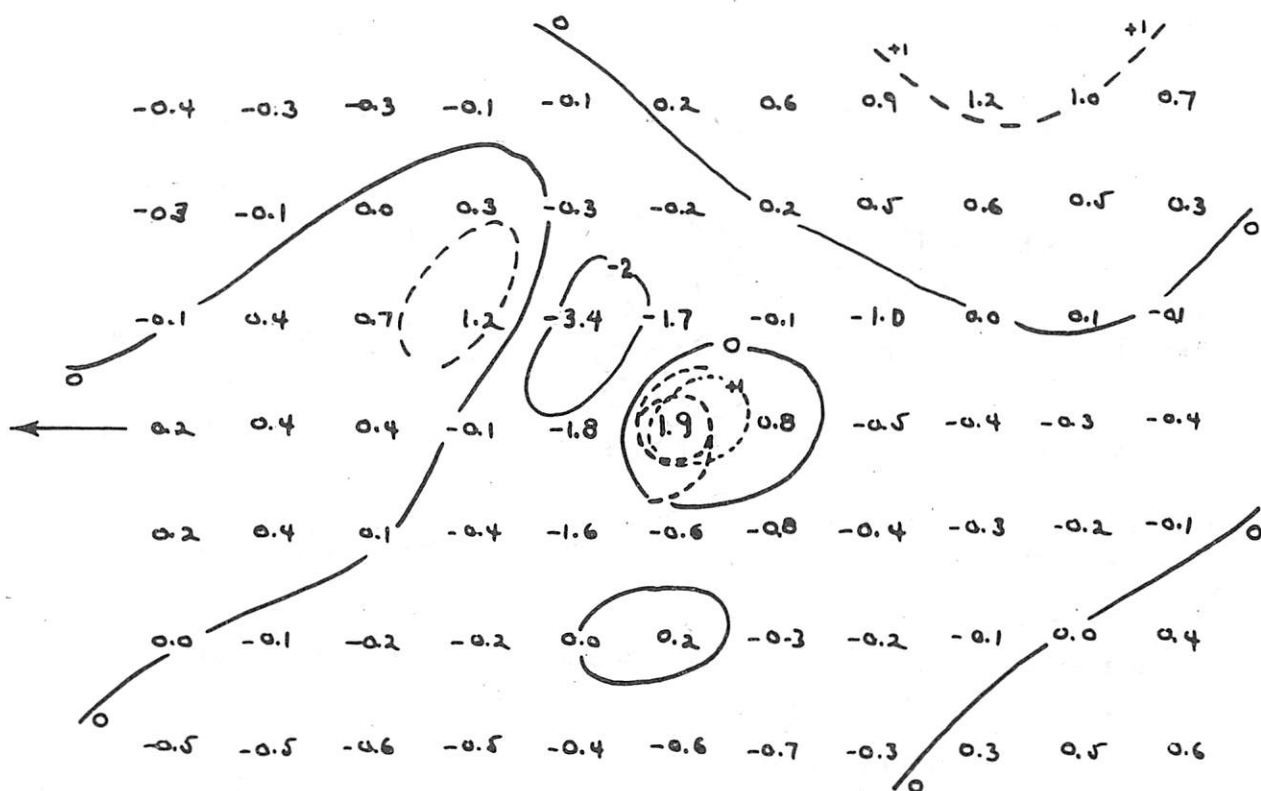
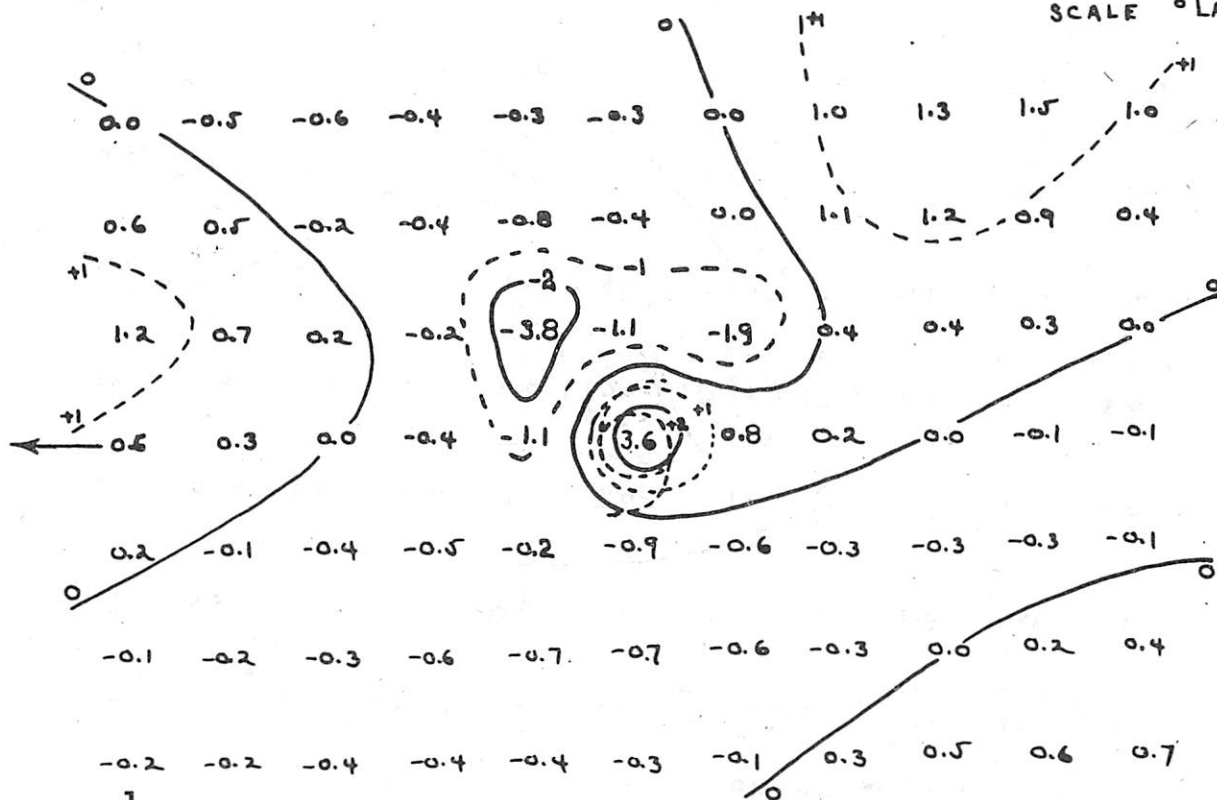


Figure 14. - Mean divergence ( $10^{-5}$  sec. $^{-1}$ ).



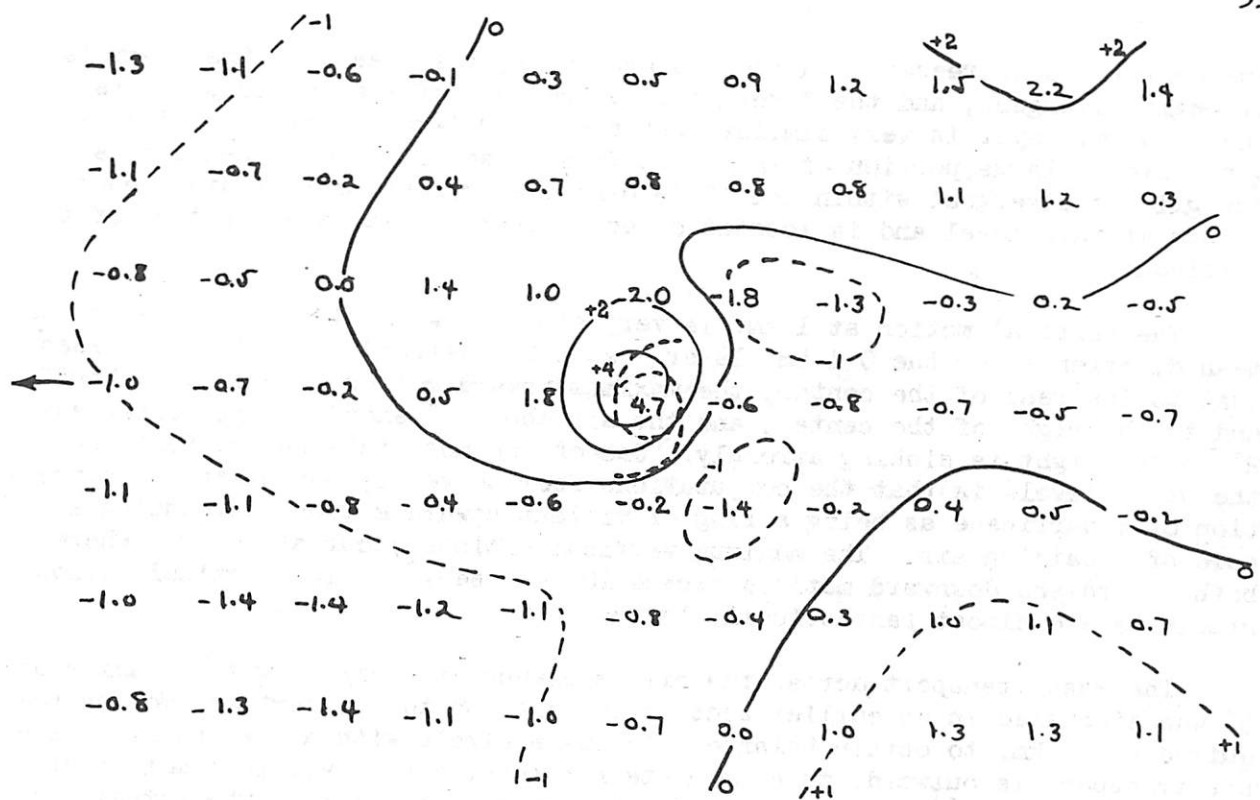
C 3-6 KM LAYER

SCALE ° LAT



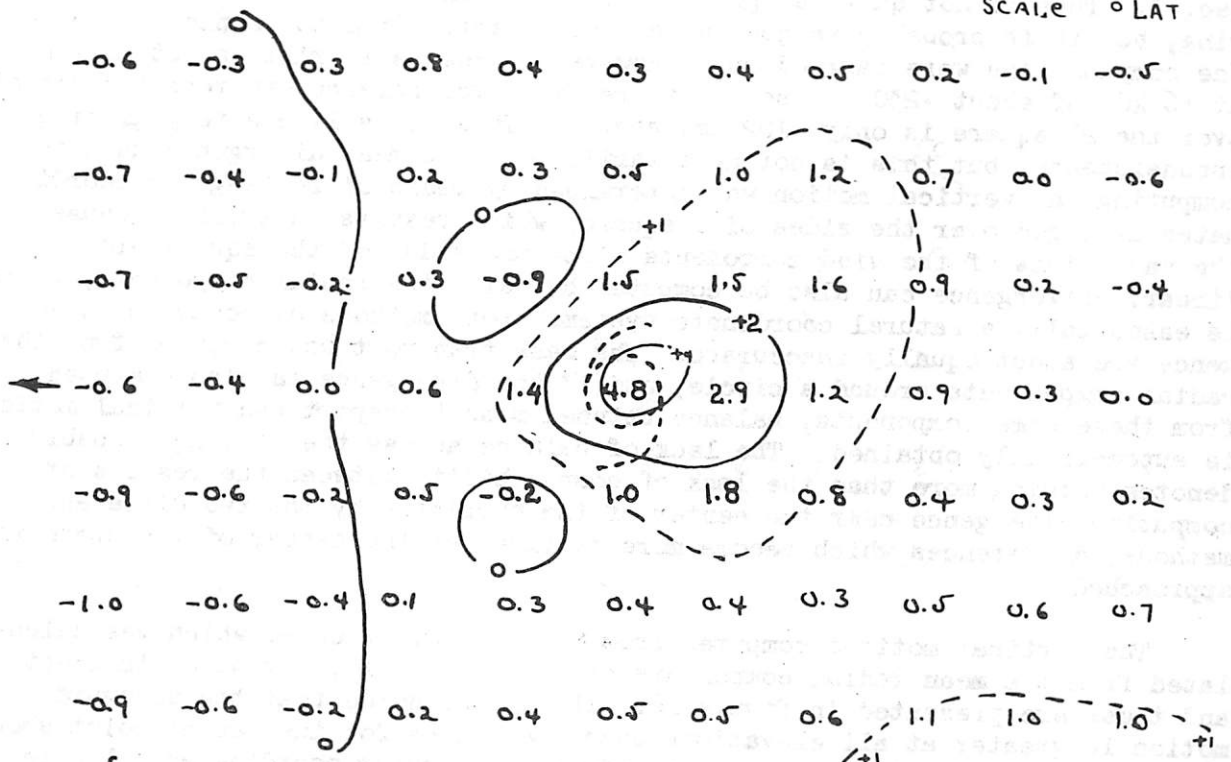
d 6-10 KM LAYER

Figure 14. - Mean divergence (continued)



e 10-125 KM LAYER

SCALE 4  
0 2 4  
° LAT



f 12.5-16 KM LAYER

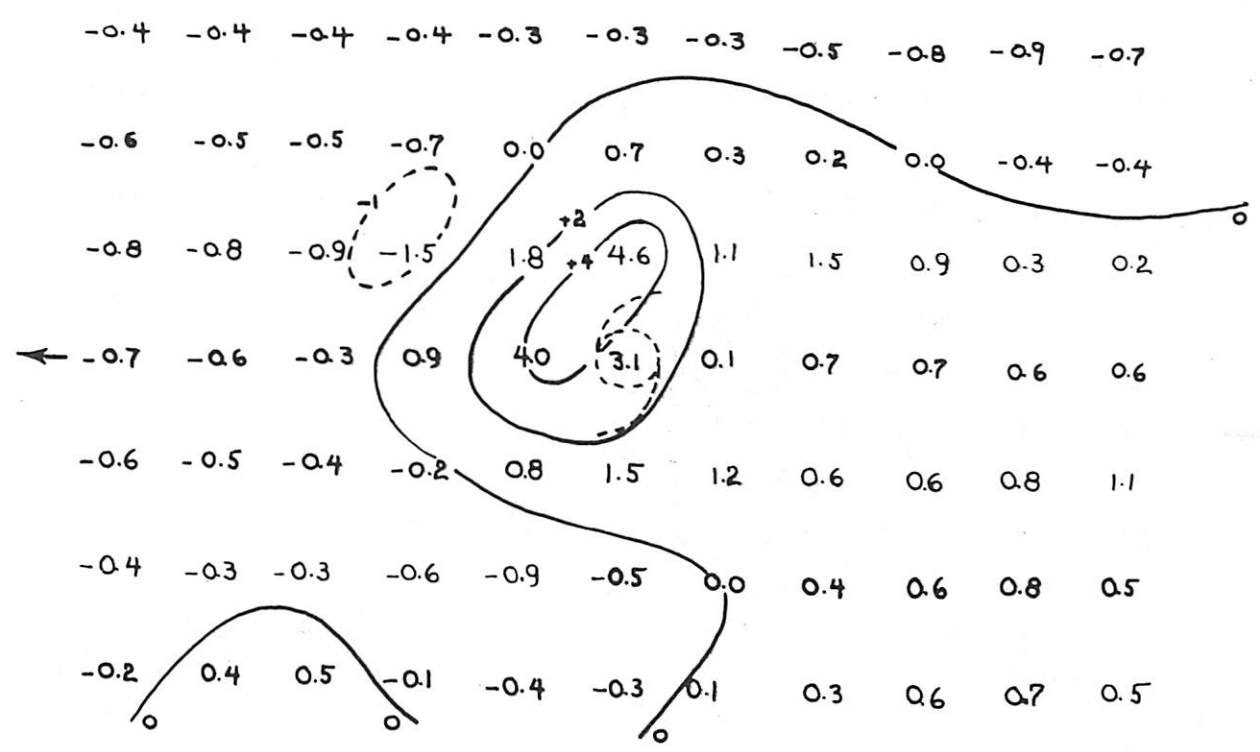
Figure 14. - Mean divergence (continued)

the center has decreased. In the 3-6-km. layer, the area over the storm is strongly divergent, and the divergence to the rear of the center persists. The 6-10-km. layer is very similar, but the 10-12.5-km. layer shows divergence over a large portion of the right front quadrant. More than one-half the grid is divergent within the 12.5-16-km. layer; the maximum divergence occurs at this level and is located directly over the surface position of the hurricane.

The vertical motion at 1 km. is very similar (with sign reversed) to the mean divergence for the 0-1-km. layer. At 3 km. descending motion is present just to the rear of the center, the maximum upward motion occurs just ahead and to the right of the center, and the air about  $4^\circ$  ahead of the center and  $2^\circ$  to the right is sinking strongly. One of the most interesting features of the upper levels is that the computations seem to verify the classical conception of a hurricane as being a ring of violent upward motion surrounding a core of subsiding air. The maximum vertical motions occur at 16 km., where both upward and downward motions exceed  $100 \text{ cm. sec.}^{-1}$ . The vertical motion gradients are almost fantastically large.

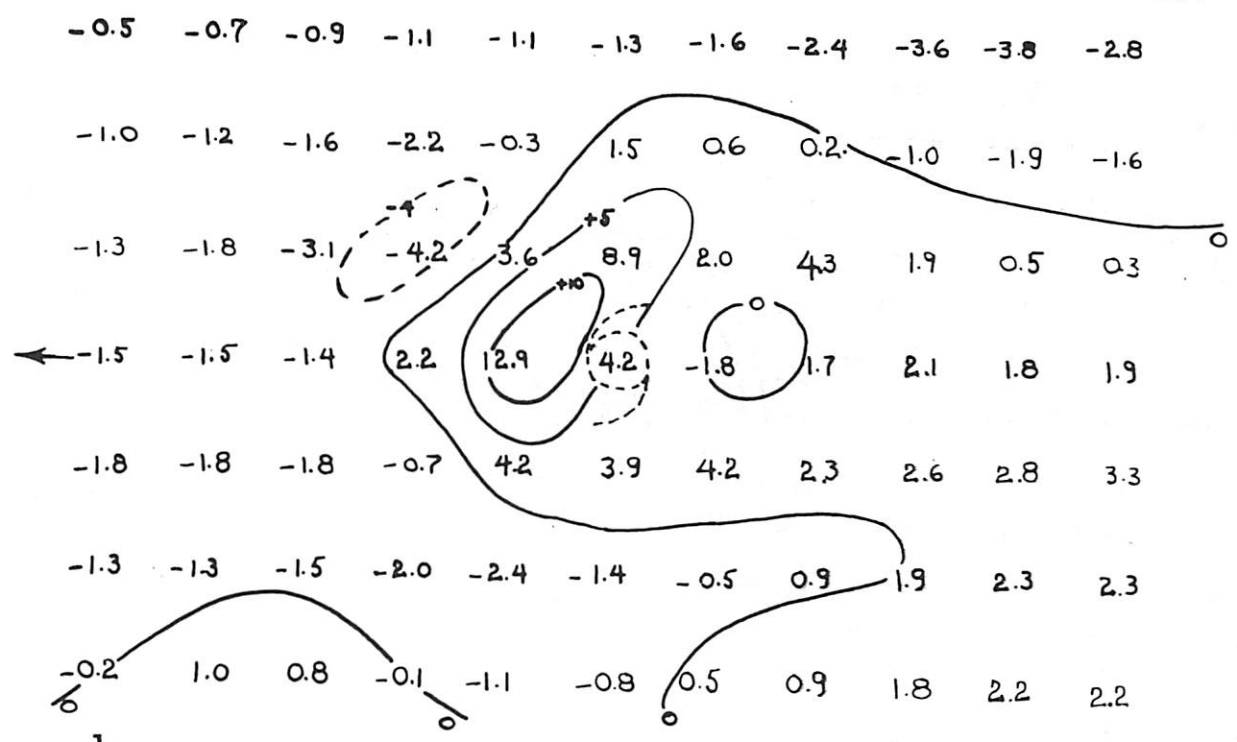
The mass transport across the circumference of a circle with a radius of  $3^\circ$  was discussed in an earlier section in relation to the vertical motion required at 16 km. to obtain balance. Across a circle with a radius of  $2^\circ$  the net transport is outward; to compensate for this, a mean vertical motion of about  $-13 \text{ cm. sec.}^{-1}$  over the area of the circle is required. The actual vertical motion (determined by weighted areas from figure 15f) is about  $-7 \text{ cm. sec.}^{-1}$ . This is not quite as good a balance as was obtained across the  $3^\circ$  ring, but it is probably as good as can be expected from the manner in which the computations were carried out. However, across a  $1^\circ$  ring, a net motion at 16 km. of about  $-230 \text{ cm. sec.}^{-1}$  is required for balance, whereas the actual over the  $2^\circ$  square is only  $-102 \text{ cm. sec.}^{-1}$ . This looks like a very glaring inconsistency, but this is not necessarily so. The mean divergence used in computing the vertical motion was determined by means of rectangular coordinates averaged over the sides of a square, which results in errors because the variations of the wind components along the sides of the square are not linear. Divergence can also be computed by using the radial components, which is essentially a natural coordinate system. Both methods of computing divergence are about equally inaccurate. The mass transport was computed from the radial components around a circle, and if the divergence is also computed from these same components, balance between mass transport and vertical motion is automatically obtained. The lack of balance across the  $1^\circ$  ring probably denotes nothing more than the lack of compatibility between the results of computing divergence near the center of the hurricane by the two different methods, differences which become more critical as the center of the storm is approached.

The vertical motions computed from the mean divergence, which was calculated from the mean radial components at a radius of  $1^\circ$ , may be of interest, and these are presented in figure 16. It will be noted that the downward motion is greater at all elevations than the values for the center point shown by figures 15a-f, which were computed from rectangular coordinates. Figure 16 shows sinking motion extends down below 3 km. These values represent



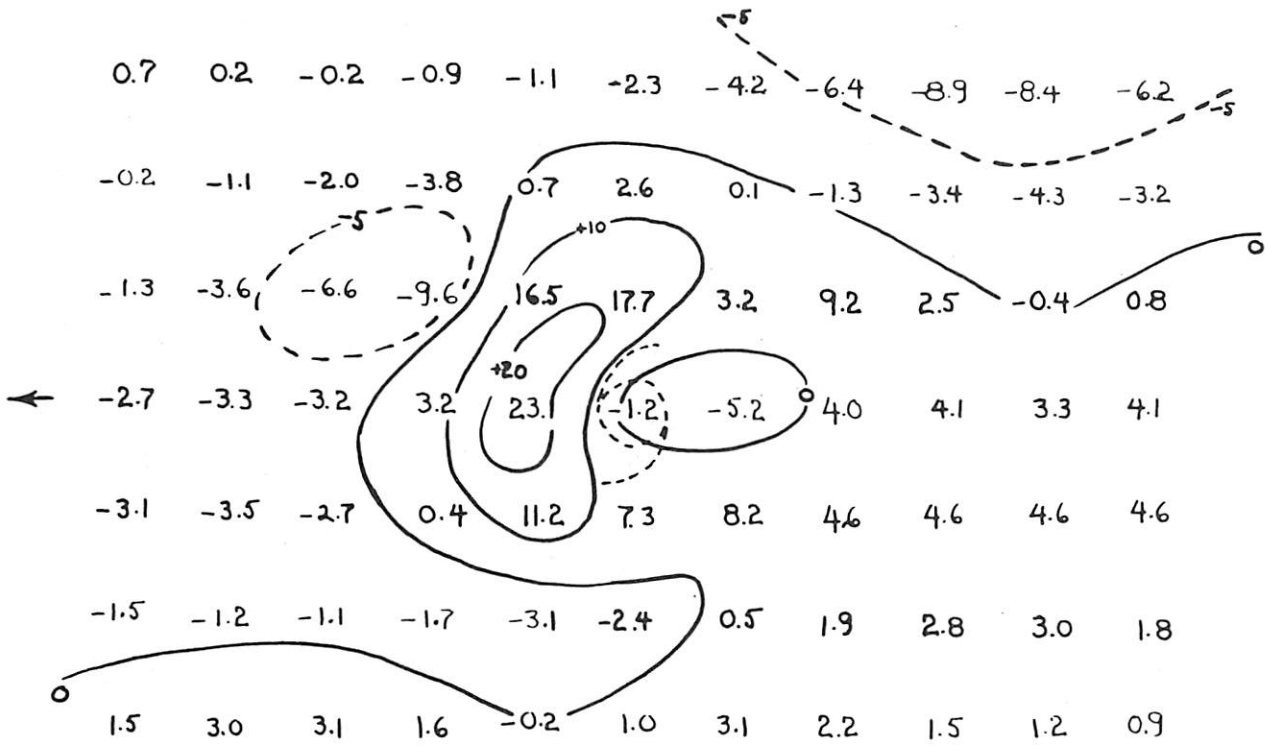
a 1 KM

SCALE 0 2 4  
° LAT



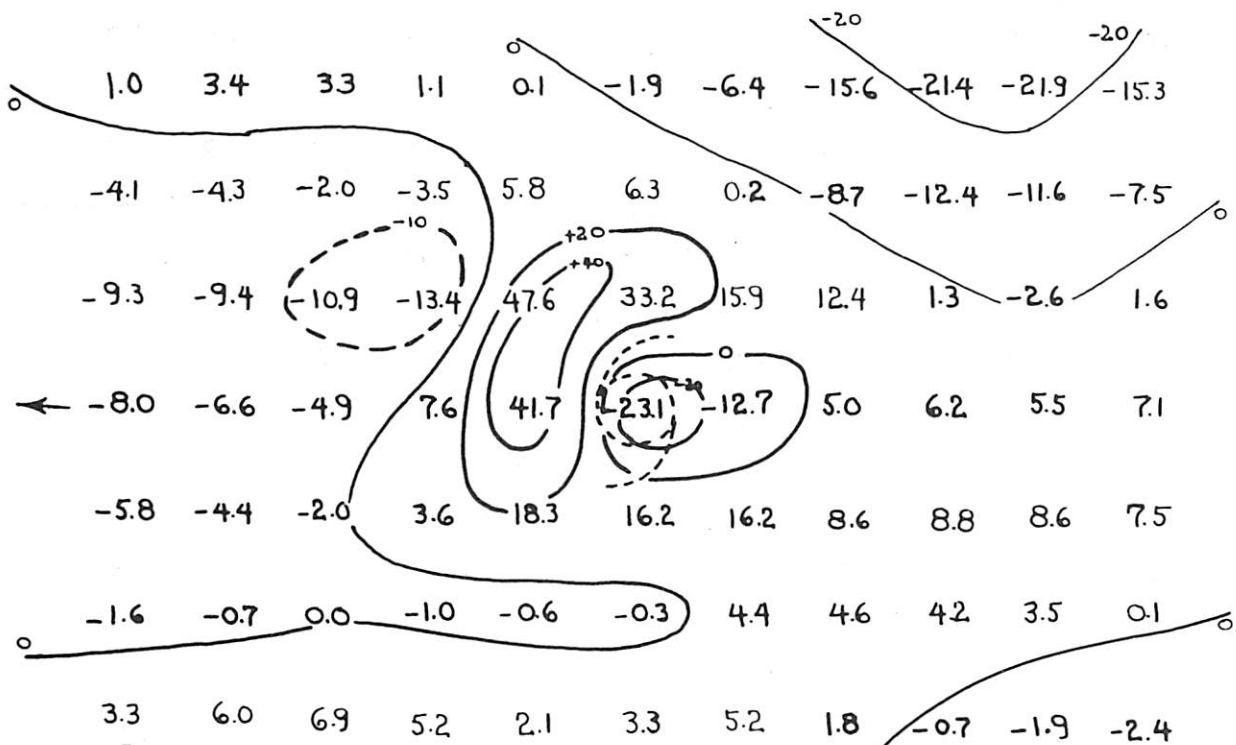
b 3 KM

Figure 15. - Vertical motion (cm. sec.<sup>-1</sup>).



C 6 KM

SCALE °LAT



d 10 KM

Figure 15. - Vertical motion (continued)

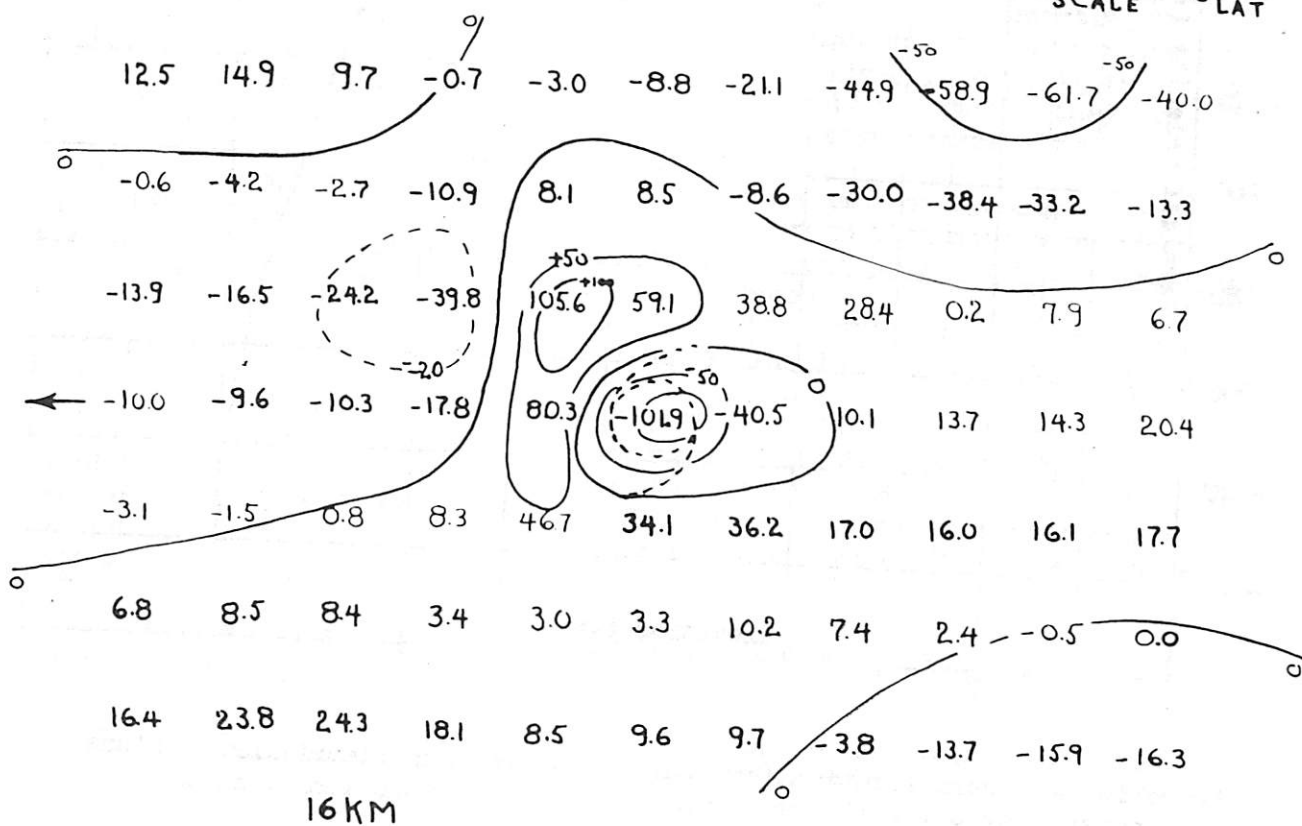
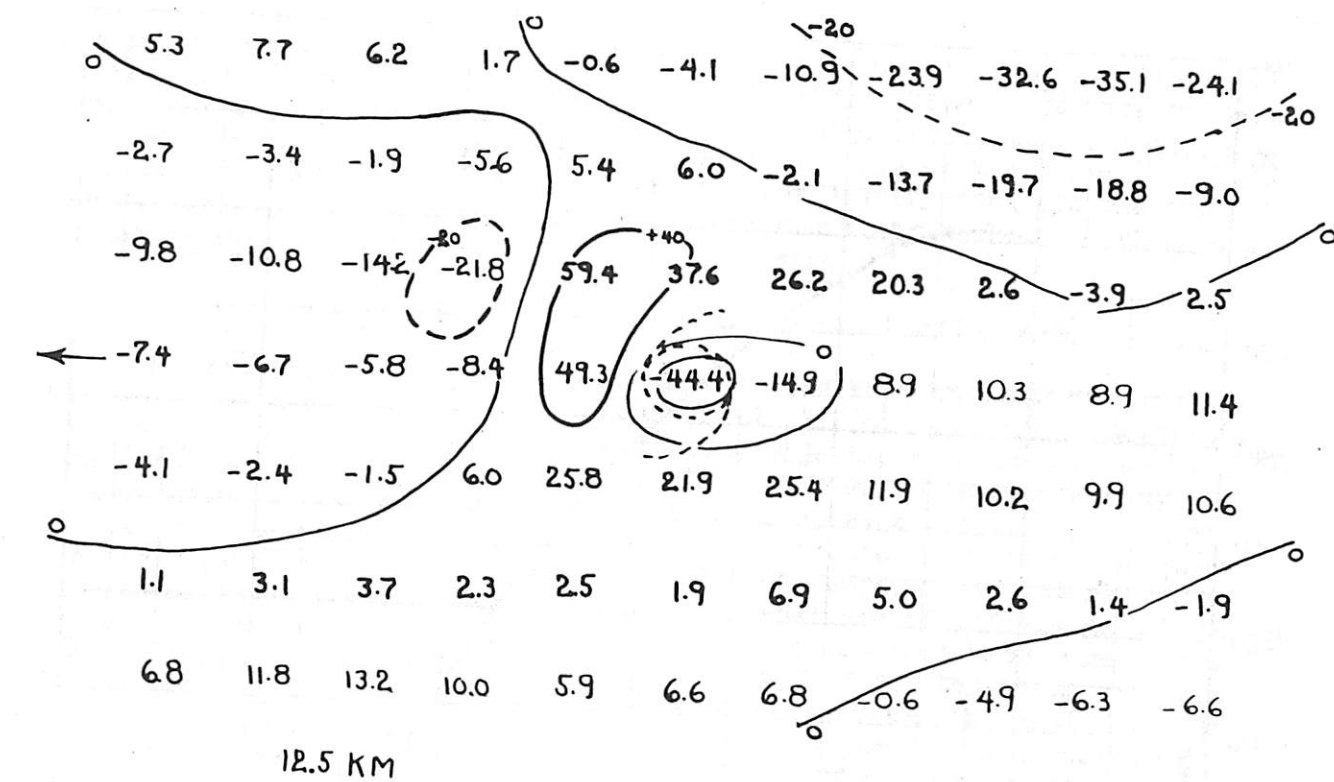


Figure 15. - Vertical motion (continued)

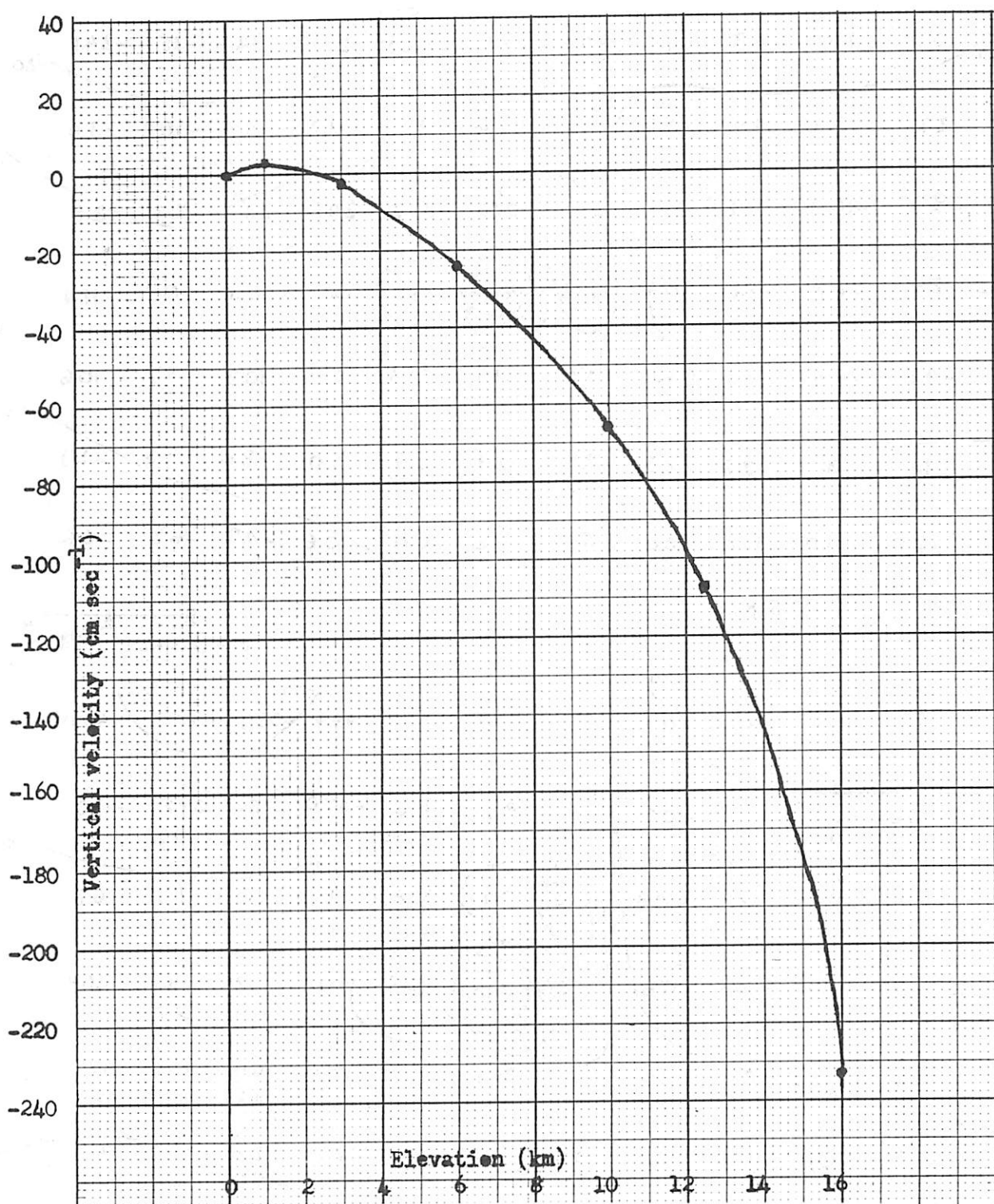


Figure 16. - Vertical motion (cm. sec.<sup>-1</sup>) at various elevations. Values computed by using the mean radial components at a radius of 1°.

a mean value for a circle with a  $1^\circ$  radius; obviously (at least in the lower levels) air is ascending within much of that circle. One is tempted to speculate that the small downward motion at 3 km. represents a much larger subsidence over the considerably smaller area of the eye of the storm, but even if such were the case, the data probably do not justify such speculation. It would, however, be compatible with the temperature structure of various eye soundings which have been made in recent years [4].

#### 11. IMPLICATIONS CONCERNING HURRICANE CIRCULATION MODELS

The data presented in the preceding sections seem to indicate that in the main, the hurricane circulations of Riehl [7] (pp. 330-339) and Simpson [8] are essentially correct, the outstanding objections being the over-simplifications they contain. Even the mean data, from which obviously many of the individual hurricane anomalies are smoothed, display a rather complicated structure. The structural variations from one tropical cyclone to another are very great, and the true hurricane model can perhaps be obtained only through an intensive observational study and analysis of individual hurricanes. During the immediate future it would seem that a detailed knowledge on the inner portions of the storm can be gained only through stepped-up aircraft reconnaissance, such as that currently being done by the National Hurricane Research Project. Studies such as that presented here can only point out clues and suggest areas where additional efforts might best be concentrated.

It is not the intent of this paper to attempt to revise existing hurricane circulation models. However, there are certain implications which may point to possible future revisions. These will be summarized below. It is not expected that all of them will be eventually verified, but rather they are suggested as regions in which future research might be concentrated.

The data indicate that there is a remarkable lack of symmetry around the storm, much of which is undoubtedly due to the motion of the cyclone itself, and it may be desirable to construct different models for the four quadrants, or at least for the right and left portions.

The vertical circulation. The vertical model should take into account the following:

1. The mean vertical motion for the  $2^\circ$  square with the eye at the center is upward from the surface up to an elevation of between 3 and 6 km., and above that height it is downward. However, subsidence is known to occur within the eye, and hence the inner portions of the storm must consist of a ring of ascending air surrounding a core of subsiding air.
2. The maximum upward motion occurs about  $2^\circ$  to the right of the direction of motion at an elevation of about 16 km.
3. Ascending motion is still occurring at 16 km. on all sides except to the rear of the center and directly over the eye. The maximum occurs around a ring  $3^\circ$  to  $4^\circ$  from the center.
4. Subsidence takes place  $2^\circ$  to  $3^\circ$  to the rear of the storm at all elevations above 1 km.

5. The strongest downward motion occurs along the outer edges of the right rear quadrant, over the eye at 16 km., and along the outer edges of the left rear quadrant.
6. Downward motion occurs at all levels about  $4^\circ$  ahead of the center and just to the right of the direction of the motion. Throughout the lowest 6 km. this center of maximum subsidence is surrounded by sinking air, but above that level ascending motion is found along the outer portions of both front quadrants.
7. Under the influence of this vertical motion pattern, multiple tropopauses should be expected around the storm. The main tropopause should be elevated in some areas and depressed in others.

The radial component. The radial motion relative to the center of the storm will be discussed here. The following are suggested as possible points for consideration:

1. The maximum inflow occurs within the 0-1-km. layer, but the data reveal radial outflow through the left rear quadrant. There is some evidence to indicate that the mean radial component decreases inside a radius of about  $2^\circ$  to  $3^\circ$  latitude.
2. The major outflow occurs above 10 km., and the mass outflow across a  $3^\circ$  ring within the 10-16-km. layer balances the mass inflow within the 0-1-km. layer.
3. There is an indication of net outflow within the 1-3-km. layer across the  $1^\circ$  ring. If verified this may indicate that the rising air is flung outward due to an excess of centrifugal force as it enters a region of weaker pressure gradient.

The tangential velocity. Little of the data concerning the tangential components differ significantly from earlier studies, but nevertheless the salient features will be summarized.

1. The velocity profile of the tangential components within the lower 1 km. followed an exponential curve of the form

$$V_t = A e^{-br}$$

where A and b are constants, r is the radial distance, and V<sub>t</sub> is the tangential velocity. Profiles for the higher layers possessed V<sub>t</sub> the same general shape, but must of necessity be expressed in a different form since the above does not permit any negative (anticyclonic) value.

2. The mean tangential components for the inner  $6^\circ$  were slightly higher through the 1-3-km. layer than they were within the 0-1-km. layer.
3. Above the 1-3-km. layer the radius and magnitude of the tangential component decreased through the remainder of the troposphere. There was, however, still evidence of a small cyclonic circulation within the 12.5-16-km. layer.

4. Anticyclonic motion predominated, however, above the 10-km. level. The maximum anticyclonic wind velocity was about 25 m.p.s., and occurred within the 10-12.5-km. layer, along the outer portions of the right rear quadrant.

#### REFERENCES

1. L. A. Hughes, "On the Low-Level Wind Structure of Tropical Storms," Journal of Meteorology, vol. 9, No. 6, Dec. 1952, pp. 422-428.
2. E. S. Jordan, "An Observational Study of the Upper Wind-Circulation around Tropical Storms," Journal of Meteorology, vol. 9, No. 5, Oct. 1952, pp. 340-346.
3. C. L. Jordan, "A Mean Atmosphere for the West Indies Area," NHRP Report No. 6, 1957, 17 pp.
4. C. L. Jordan, "Mean Soundings for the Hurricane Eye," NHRP Report No. 13, 1957, 10 pp.
5. H. A. Panofsky, "Methods of Computing Vertical Motion in the Atmosphere," Journal of Meteorology, vol. 3, No. 2, June 1946, pp. 45-49.
6. H. A. Panofsky, "Large-Scale Vertical Velocity and Divergence," Compendium of Meteorology, American Meteorological Society, Boston, Mass. 1951, pp. 639-646.
7. H. Riehl, Tropical Meteorology, McGraw-Hill Book Co., Inc., New York, N. Y., 1954, 392 pp.
8. R. H. Simpson, "On the Structure of Tropical Cyclones as Studied by Aircraft Reconnaissance," Proceedings of the UNESCO Symposium on Typhoons, 9-12 Nov. 1954, Tokyo, 1955, pp. 129-150.